Author version: *Environ. Sci. Technol., vol.48; 2014; 11343-11351*

Source investigation of the tar balls deposited along the Gujarat coast, India, using chemical fingerprinting and transport modeling techniques

V. Suneel[1], P. Vethamony[1*], B. G. Naik[1], K. Vinod Kumar[2], L. Sreenu[3], Samiksha. S. V[1], Yunus Tai[4], K. Sudheesh[1]

[1]CSIR-National Institute of Oceanography, Dona Paula, Goa 403004, India

[2] Tropical Marine Science Institute, National University of Singapore, 14 Kent Ridge Road, 119 227, Singapore

[3]CSIR-National Institute of Oceanography, Visakhapatnam, Andhra Pradesh, India

[4] Gujarat Pollution Control Board; Sector-10-A, Gandhinagar, Gujarat-382 010

[*]**Corresponding author:** P. Vethamony, CSIR-National Institute of Oceanography, Dona Paula, Goa 403 004, India. Email: mony@nio.org, Tel +91 832 2450473; Fax No. +91 832 2450608

Abstract

Deposition of tar balls (TBs) along the south Gujarat coast, situated on the west coast of India (WCI), commonly occurs during the southwest monsoon season. Several offshore oil fields off Mumbai-Gujarat coast, and refineries along the coast might be sources of oil spills/leakages and lead to the formation of TBs. To identify the sources we collected twelve TB samples from the beaches of Gujarat (Tithal, Maroli, Umbergam and Nargol) during 15-17 July 2012 as well as samples of crude oils, namely, Cairn (CRN), NIKO (NIK), MSC Chitra (MSC) and two at Bombay High (BH). These TBs were subject to the following multimarker approach for source identification: Diagnostic Ratios (DRs) of n-alkanes, polycyclic aromatic hydrocarbons (PAHs), pentacyclic triterpanes, compound specific isotope analysis (CSIA), Principle Component Analysis (PCA) and numerical simulations (hydrodynamic model coupled with particle trajectories). The chemical fingerprint results reveal that the source of the TBs is BH crude oils, and the model results confirm that the source location is BH north oil fields (BHM). This is the first study of its kind in India to use fingerprinting and transport modeling techniques for source identification of TBs.

Keywords: tar ball, fingerprinting, n-alkanes, PAH, hopanes, biomarkers, Diagnostic ratios, Gujarat, Hydrodynamic, Bombay High

1. Introduction

The West Coast of India is prone to receive TB deposits during the southwest monsoon season (SWM). During this season, the TB deposits frequently affect the northern part of WCI (Gujarat coast). TB is the residue of oil spill washed to seashore, which is remnant of source oil, after physical, chemical and biological processes, called weathering in the sea. Deposition of TBs on the beaches could affect the marine ecosystem, the recreational activities and hence the tourism. Therefore, identifying their sources is highly essential inorder to find out the remedy for cause and to mitigate the oil pollution in the region. Gujarat has the longest coastline (≈1600 km) in India, and has several crude oil related industries and ports along the two gulfs- Gulf of Kachchh and Gulf of Khambhat (GoK). There are also many offshore oil fields: belonging to Cairn Energy, Niko resources, BH oil fields. Refineries, fertilizer, chemical and cement industries, power plants, minor and major ports and salt works are the major industries located along the Gujarat coast; more than 10 Single Point Moorings (SPMs) are installed off Gujarat coast; Gujarat has 6 shipbuilding yards and more than 50 ports; the ports at Okha, Navlakhi, Kandla, Mandvi and Jakhau handle a variety of cargos, especially petroleum products. In 2011-12, the ports in Gujarat handled 259 million tonnes of cargo, which was the highest compared to previous years, indicating growth of industries and traffic. In addition to these, oil spills could also occur along the international tanker route (Fig.1a) due to tanker washes, collision and grounding of tankers/ships; hence, oil leakages followed by TB formation may be possible, such as occurred after an oil spill accident off Mumbai on 07 August 2010 due to the collision of two ships MV Khalijia-111 and MSC Chitra causing a spill of 400 tonnes of oil. Finding the source of TBs is essential in order to mitigate oil pollution as well as TB deposition. In this context, we have carried out sampling of TBs along the Gujarat coast during July 2012 for fingerprinting.

Several studies have been carried out in order to fingerprint TB/oil spill throughout the world, but a limited number of studies are available in India. Biomarkers play a key role in environmental forensics. They are derived from the dead bodies of formerly living organisms present in the source rock of oil produced and contain the same structure of parent organic molecules. The DRs pentacyclic terpanes, n-alkanes, PAHs are widely used in oil fingerprinting studies. The homohopane index C_{29}/C_{30} and $\sum C_{31}$-C_{35}/C_{30} is a more reliable source identifier for oil spill fingerprinting[1-2]. The most used other DRs are tricyclic C_{23}/C_{24}, C_{29} αβ/ C_{30} αβ hopane, Oleanane/ C_{30} αβ hopane, T_s/T_m, and $T_s/(T_s + T_m)$[3]. Recently, Mulabagal et al.[4] have fingerprinted the TBs that are deposited along the Alabama shoreline using the DRs of hopane compounds such as Ts/Tm, $C_{29}\alpha\beta/C_{30}\alpha\beta$,

C_{31}(22S)/C_{31}(22S+22R), C_{32}(22S)/C_{32}(22S+22R), C_{33}(22S)/C_{33}(22S+22R), C_{34}(22S)/C_{34}(22S+22R), and C_{35}(22S)/C_{35}(22S + 22R) ratios. DRs of PAHs and n-alkanes, Flu/Flu+Pyr, Phe/Ant and Pr/Py, C_{17}/Pr, C_{18}/Py and C_{17}/C_{18} are also support tools to source identification and to estimate the rate of weathering.[5-8] However, the results obtained by the DRs of alkanes, PAHs and hopanes may not be good enough to fingerprint the source, as ambiguities still exist, and in such cases CSIA is preferred, as it is a powerful tool to confirm the source. CSIA is widely used in marine environmental studies mainly to track the sources. The isotope ratios cannot be altered by weathering effects. For example, Macko et al.[9] observed only 0.5‰ difference in the $\delta^{13}C$ values after 2 years of weathering. The short term weathering processes such as evaporation and dispersion cannot affect the carbon isotope composition ($\delta^{13}C$) values of individual n-alkanes.[10,11] Though weathering causes loss of volatile compounds, $\delta^{13}C$ values of non-volatile and semi volatile compounds are unaffected by weathering and their isotopic ratios can be used to trace the oil spill sources[12]. Stable isotopes are resistant to decay over geological time scales and widely used for source identification and fingerprinting.[13] Suneel et al.[8] identified the source of TBs deposited along the Goa coast as South East Asian Crude Oil (SEACO) based on the CSIA ($\delta^{13}C$).

All the above studies are based on chemical methods. Though research work on TBs started in the 1970s, there still exists a gap in understanding their transport phenomenon on the WCI. The concentration of floating TBs in the Western Pacific from Tokyo to north of Hawaiian Island was 14 mg/m^2 with an average of 3.8 mg/m^2 [14] and these tar residues are formed due to tanker washes along the tanker route (Arabian Gulf to Japan).[15] Lebreton et al.[16, 17] used a global circulation model coupled with particle-tracking to simulate the transport of floating debris. Martinez et al.[18] studied the drift mechanism of floating marine debris in the Pacific Ocean. They found that floating debris accumulates to the convergence zone due to Ekman drift and geostrophic currents. Suneel et al.[19] simulated trajectories of TB transport to the Goa coast using the MIKE21 hydrodynamic modelling coupled with particle analysis. In this study also, we have used the same suit of models to study the circulation pattern, and find the probable origin and trajectories of the TBs deposited on the south Gujarat coast.

The primary aim of the present study is to fingerprint the TBs that were deposited along the south Gujarat coast and to confirm the source location by using a Hydrodynamic model (HD) coupled with a Particle Analysis (PA) model. In order to fingerprint the TBs we have used the DRs of n-alkanes, PAHs, pentacyclic triterpanes, in conjunction with the CSIA for 12 TB samples (collected off south

Gujarat coast), and five crude oil samples (expected sources). This is probably the first study in India to identify the source of the TBs using fingerprinting, coupled with transport modelling.

2. Experimental Section

2.1. Sample collection

We collected twelve TB samples from four beaches Nargaol (NB1, NB2) and Umbergaon (UB1, UB2) on 15 July 2012 and Maroli (MB1, MB2), Tithal (TB1, TB2), Nargaol (NB3, NB4) and Umbergaon (UB3, UB4) on 17 July 2012. Samples were collected and kept in glass bottles and stored in the laboratory refrigerator prior to the analysis. We also collected the following crude oil samples: (i) two Bombay High based crude oils. BH oil fields are located $\approx$ 250 km away from the tar ball sampling points (Gujarat coast). The crude oils produced from various platforms of BH reach the Uran plant through two main pipelines - 30$^{''}$ MUT (Mumbai High Uran Trunk) oil pipeline from the BH and 24$^{''}$ HUT (Heera Uran Trunk) oil pipeline from the Heera offshore Platform, (ii) two crude oil samples from Cairn and Niko oil fields, off Gujarat coast and (iii) one crude oil sample from the vessel MSC Chitra (MSC) - grounded after collision with MV Khalijia-III on 07 Aug 2010, off Mumbai coast. Fig. 1 shows the tar ball sampling locations and crude oil well locations.

2.2. Extraction and Chemicals

Crude oil and TB samples were weighed precisely 20 mg and 30 mg, respectively. Detailed analytical processes and fractionations are given in Supporting Information SI. 1. Authentic standards for alkanes and PAH (Sigma Aldrich, USA) and hopane standards 17β (H) 21α (H)-hopane (C_{30}17βα), 17α (H) - 22, 29, 30- trisnorhopane (Tm) (Chiron, Norway) were used.

2.3. Gas Chromatography-Mass spectroscopy (GC-MS) analysis

Analyses for *n*-alkane, Sterane and Hopanes for TBs and crude oil samples were performed using a Shimadzu QP-2010 Gas Chromatograph and Mass Spectrometer interfaced with AOC-20i auto sampler. For GC-MS specifications, peaks identification and quantification, see section SI. 2, Supporting Information.

2.4. Gas Chromatography-Isotope Ratio Mass Spectroscopy (GC-IRMS)

Carbon isotopic ratios of individual n-alkanes have been determined on Agilent 7890 A GC-C-IRMS coupled with Agilent 7000 GC-MS triple quad interfaced with oxidation-reduction reactor (980-

650^{o}C). The specifications for GC-IRMS and quantification procedure are given in section SI. 3, Supporting Information.

2.5. Model set-up and Principal Component Analysis (PCA)

The MIKE 21 HD model coupled with PA model was used to compute hydrodynamics (describing water velocities) of the model domain (67^0 - 73.5^0E and 16.5^0 - 24. 16^0N) (Fig. 1b), and for generating TB trajectories. The HD model has been widely used at CSIR-NIO by researchers for simulating coastal hydrodynamics, DO-BOD, spill movement, fish and barnacle larvae transport, estimation of residence time of pollutants, sediment transport and effluent dispersion (Babu et al.[20,21] Vethamony et al.[22,23] Grinson et al.[24] Chetan et al.[25] Rupali et al.[26] Samiksha et al.[27]). The bathymetry data are generated from the combined data of MIKE-CMAP and modified ETOPO 5.[28] A brief description of the models and PCA is given in the section SI. 4, Supporting Information.

Fig. 1. to be inserted here

3. Results and Discussion

3.1. Alkane fingerprints

The Isoprenoid alkanes such as Pristane and Phytane can get altered by the effect of biodegradation. Hence, the ratios C_{17}/Pr and C_{18}/Py significantly decrease when biodegradation takes place. If the samples have undergone weathering by a biodegradation process, a hump usually appears in the GC chromatogram called Unresolved Complex Mixture (UCM). Results show that UCM is observed slightly in all TB samples (see Fig. S4, Supporting Information). DRs of n-alkanes- Pr/Py, C_{17}/Pr, C_{18}/Py and C_{17}/C_{18} are calculated for all the samples of TB and crude oil. The ratios of TB samples are nearly the same, suggesting that the source may be the same for all samples. The ratio of C_{17}/Pr for all the TB samples (BHM, BHH, NI, CRN and MSC) is in the range of 0.68-0.91 (0.96, 0.94, 1.78, 1.71 and 5.97) and C_{18}/Py is in the range of 3.56-4.42 (4.81, 5.67, 9.85, 9.83), indicating that the samples were weathered significantly. The UCM is also present in all the TB samples. Therefore, it is prudent to state that TBs are weathered moderately in various degrees due to biodegradation. TBs derived from tanker washes are in abundance of higher molecular weight n-alkanes with the absence of UCM.[2] Therefore, the presence of UCM and lower ratios of Pr/Py when compared to unweathered crude oils suggest that the TBs had not originated from tanker washes. The Carbon Preference Index (CPI) is often used to estimate the thermal maturity of the petroleum, and it is generally 1.0 for petroleum[29]. The calculated CPI for all TB samples is in the range of 1.18-1.19,

which shows that TBs are derived from the petroleum products. The ratios of L/H are in the range of 0.79-1.25, whereas for crude oils: BHM-1.53, BHH-1.37, NIK-1.77, CRN-3.10, MSC- 3.03 (Table S4, Supporting Information). It may be noted that L/H ratios of TBs are lower than those of crude oil because the lower molecular weight components have weathered due to evaporation and biodegradation, and different ratios suggest that samples were weathered in various degrees.

Wang et al.[30] developed the Weathering Index (WI): WI decreases with increasing weathering of low molecular weight n-alkanes. We notice that WI of TB samples in various degrees (0.08-0.16). Low concentration of phytane is observed in all TB samples, and this is not because of weathering effect but may be due to source oil characteristics as all the crude oils BHM, BHH, CRN, NIK and MSC also have the same characteristics. The ratio of Pr/Ph for TB samples is in the range of 4.22 - 4.77, whereas, for BHM, BHH, NI and CRN, the ratio is 4.99, 6.03, 5.56, 6.38, respectively, showing that ratios of TBs are much closer to the ratio of BHM; hence, the source could be BHM. The ratios of Pristane and Phytane are used as indicators of source rock depositional environment: Pr/Ph<1 indicates anoxic environment, Pr/Ph =1 indicates alternating oxic and anoxic conditions, whereas Pr/Ph>1 indicates oxic condition. In the present study, Pr/Ph is > 1.0 for all TB samples and crude oils, indicating that crude oils might have been derived from source rocks, deposited in oxic conditions.

3.2. PAH fingerprints

PAHs are major constituents of crude oil (petrogenic origin), and they also form due to incomplete combustion processes of organic matter (Pyrolitic origin) biological and physicochemical alteration of organic matter that occur in sediments (diagenetic origin)[12]. Methyl Phenanthrenes (MPs) such as 3, 2, 9 and 1 are useful to differentiate the crude oils. In the present study, we find that 3, 2 and 1 MPs are less abundant than the 9 MP for all tar balls and BHM and BHH crude oil samples, whereas for MSC, CRN and NIK crudes, it is different suggesting that the source oil could be either BHM or BHH crude oil. Normally 3, 2, and 1 MPs are less abundant than the 9 MP in crude oils, and the reverse is true in the case of heavy fuel oils.[31, 32]

The parent PAHs and their DRs such as Phe/Ant, Ant/Ant+Phe, BaA/BaA+Chr, Fth/Fth+Pyr, IcdP/IcdP+BghiP, Fth/Pyr have been widely used for source identification.[33, 5, 6, 34] We have computed the same DRs for all the samples (See Table S5, Supporting Information). The results show that the ratios of MSC, CRN and NIK are not corresponding with the TBs, whereas, the ratios of BHM are very near to those of TB samples, suggesting that the source may belong to BH crude

oil. However, we cannot confirm the same only with the DRs of USEPA-16 PAHs. The Alkylated PAHs and DRs of their homologue groups have been recognized as useful tools in the field of oil spill/TB fingerprint and widely used for source confirmation. In this study, the homologue groups of naphthalene, chrysene, phenanthrene, flourene and dibenzothiophene are analyzed and the results are illustrated in Fig. S5, Supporting Information. The Fig. S5 shows that all the TBs have identical pattern, indicating that the source might be the same. The abundance of phenanthrene and chrysene in samples relative to the others indicates that they are derived from the Bunker C fuel.[29] The present analysis shows that the naphthalene homologue groups are abundant in the collected samples, and the samples are neither weathered nor belonging to Bunker C fuel. The double plot ratios C2D/C2P to C3D/C3P are widely used to identify the major PAH sources in sediment, biological PAHs, combustion product PAHs, natural petrogenic PAHs.[35, 36] In this study, we could not calculate these ratios due to technical problems, but based on the results of PAH analysis, it is possible to say that samples are derived from the petrogenic, particularly from crude oil and the source is the same for all samples.

3. 3. Source Specific Biomarkers

Biomarkers are widely used in oil spill fingerprint and environmental forensic studies as they are highly resistant to weathering.[30, 37, 1, 2, 7, 8] Crude oil formed in different geological time scales unveil a unique biomarker fingerprint. Thus, the chemical analysis of biomarker plays a prominent role in fingerprinting of TBs. In this study, we used pentacyclic triterpanes (C_{29}-C_{35}) including oleanane. Pentacyclic triterpanes having large thermodynamic stability and resistant to biodegradation. Biomarkers of terpane compounds generate information in determining sources. The hopane DRs of C_{29}/C_{30} and homohopane index $\sum(C_{31}–C_{35})/C_{30}$ widely used as molecular tools to distinguish the source of petroleum. In order to fingerprint the TBs that were deposited along the Gujarat coast, we have used biomarker diagnostic indices. We found that the TB samples and crude oils (BHM, BHH, CRN and NIK) are enriched in C_{30}(17α(H),21β(H)-hopane) and their chromatograms are also apparently the same, mounting suspicion about the source of TBs - BHM, BHH, CRN or NIK, whereas for MSC it is different. The homohopane distribution that can be used for correlation between samples,[38] also suggests that the MSC is quite different from all other crude oils, and TBs followed more or less the same pattern of other crude oils (Fig. S6, Supporting Information). Therefore, confidently, we can state that MSC is not the source oil. The chromatograms of TBs resemble BHM (See Figs. S7 and S8, Supporting Information). But a keen observation shows that Oleanane is abundant in BHM crude oil compared to other crude oils. Oleanane is a compound that

is usually observed in crude oils that are produced by plant material deposited in the deltaic environment[39]. This specific property is therefore helpful in identifying the source of anonymous oil spills. The presence of Oleanane is an indicator of tertiary or late cretaceous source rock with terrigenous influence.[40] The samples BHM, BHH, CRN and NIK are also abundant in Oleanane, showing that they belong to the tertiary or late cretaceous source rock. All the TB samples also contain significant amount of Oleanane, giving evidence to our suspicion. The crude oils that were produced in marine shale, carbonate and marl source rocks have higher $C_{31}R/C_{30}$ hopane(>0.25).[38] All the 5 crude oils and 12 TB samples which were analyzed in this study have the ratio > 0.25 (Table S6, Supporting Information), confirming that the source oils are produced in the marine shale (CRN, NIK, BHM and BHH are produced in the marine environment in the shelf region off Gujarat). The ranges/values of different DRs for TB and crude oil samples are given in Table S6, Supporting Information. The DRs of TBs are very near to the BHM ratios. The ratios of T_s-18α(H),21β(H)-22, 29, 30-trisnorhopane and T_m-17α(H),21β(H), 22, 29, 30-trisnorhopane are indicators of maturity or source inferences of oil.[41] These values show the level of maturity, and the values are more or less similar. T_m is less stable than T_s, the ratio $T_s/T_m<1$ suggests a lacustrine/saline, marine evaporatic or marine carbonate depositional environment.[42]

The DRs of Pentacyclic triterpanes C_{29}/C_{30} and $\sum C_{31}$-C_{35}/C_{35}, called homohopane index, are reliable source identifiers.[2] The cross plot between the DRs C_{29}/C_{30} and $\sum C_{31}$-C_{35}/C_{35} clearly indicate that MECO, SEACO and MSC (red, pink and green circles in Fig. 2) do not correspond with the TBs. Nevertheless, BHM and BHH crude oils meticulously match with the TBs (black circle in Fig. 2). The ranges of CRN and NIK are also very close to the TBs (orange circle in Fig. 2). The Homohopane index cross plot conspicuously reveals that MECO, SEACO and MSC crudes are not the sources for the formation of these TBs. Thus, based on the DRs of alkane, PAH and pentacyclic triterpanes, the source of the TBs appears to be the BH crude oils. However, the hopane DRs of CRN and NIK are close to the DRs of TBs. Therefore, in order to confirm the source of TB, we performed another diagnosis - the compound specific isotope analysis - for TB samples and crude oils.

3. 4. Compound Specific Isotope Analysis (CSIA)

The CSIA is one of the techniques often used in fingerprint of spills or TBs. Macko et al.[43] studied the stable Nitrogen and Carbon isotope ratios and identified the sources of beach tars as natural seepage, spills in the transport, off-loading of cargo or the disposal offshore of bilge oil. Murray et al.[44] illustrated the $\delta^{13}C$ ratios for different tertiary crude oils using CSIA for n-alkanes. They pointed out an interesting feature in the slope of the $\delta^{13}C$ alkane line with increasing alkane size. The slope is

steep in fluvio deltaic oils, whereas in most of the lacustrine, marine deltaic and marine carbonate oils it is shallower or flat. In the present analysis, the slope is steep and higher molecular alkanes are isotopically lighter than the lower molecular alkanes. Mansuy et al.[10] confirmed that GC-IRMS is a more powerful tool to correlate the samples for the source oils. In this study, we find that $\delta^{13}C$ ratio lines of BHM and BHH are virtually identical to each other. The CRN and NIK also apparently follow identical patterns (Fig. 3).

Fig. 3. To be inserted here

This is because the BHM and BHH are generated from the same type of source rock and produced in the BH basin fields. Therefore, the $\delta^{13}C$ ratios are same for these two crude oils. Likewise, CRN and NIK are also produced offshore off the coast of Gujarat. The distance between these two wells is not more than 10 km; therefore, the produced crude oil characteristics of both sources can be identical. However, apparently there exists a difference between BH based crude oils and CRN and NIK crude oils. The $\delta^{13}C$ ratios of lower molecular components (C_{15}-C_{26}) of BH based crude oils are isotopically higher compared to those of CRN and NIK crude oils, while the $\delta^{13}C$ ratio of higher molecular components (C_{26}-C_{35}) are lighter, but close to each other. The case is the reverse for MSC crude oil. The $\delta^{13}C$ ratios of alkanes beyond C_{20} are isotopically heavier than TBs and BH, CRN and NIK crude oils. Therefore, we confirm that MSC, CRN and NIK crude oils are not the sources for the TBs deposited on the Gujarat coast. There exists a good match between BH based crude oils and the TB samples; alkane $\delta^{13}C$ ratios follow the same pattern and within the range of both the crude oils and TBs. Thus, CSIA analysis confirms that the source of the TBs is BH based crude oil (either BHM or BHH).

To confirm the source more specifically additional PCA has been carried out. Utilizing the eigen value criterion, two factors were chosen as principal factors which explained about 88% of the total variability in the carbon isotope data of TB samples and crude oils. The biplot between these two components is given in Fig. S9, Supporting Information. Fig (S9) shows that MSC and CRN crude oils, to a large extent, are far away from the remaining samples, and clearly suggest that they are not the source candidates. Apparently, NIK and BH crude oils have similar characteristics. A review work by Hunt et al.[45] reveals that the combination of biomarker and stable isotope analysis can be used as a tool for source correlation in the field of petroleum geochemistry. Thus, based on the triterpane and CSIA analyses the source belongs to BH crude (either BHH or BHM), and the n-alkane and PAH DRs of TBs correlate with the BHM crude. In order to confirm the probable origin locations, we have simulated TB trajectories using HD model coupled with PA model.

4. Modelling: hydrodynamics and particle tracking

The Indian Ocean experiences seasonal reversal of winds - SWM during June to September and northeast monsoon (NEM) during November to February. SWM is the stronger and during this season, strong winds prevail over the Arabian Sea (AS), and directly hit WCI. The reversal of wind pattern builds up the circulation in the north Indian Ocean. Therefore, surface currents in the AS are due to combined effect of wind driven Ekman drift and geostrophic currents.[46] In order to understand the circulation and particle transport, we performed four experiments during April, May, June and July.

In the numerical experiment, particles weighing 5g were released at probable locations. We find that TBs deposited along the Gujarat coast during 15-17 July 2012 were in the range of 2-4 cm diameter. According to Sontro et al.[47] TBs of 3 cm in diameter and 0.405 cm in thickness would contain a mass of approximately 5.96g. Based on this calculation, TBs of mass 5g should have a diameter of 2.516 cm; this value reasonably matches with the range of diameter of the TBs deposited along the Gujarat coast.

4. 1. Winds and currents in the domain

The monthly averages of ECMWF winds used in the study depicts that the weak northwesterlies prevail in April, moderate westerlies in May and strong southwesterlies in June and July (Fig. 4) matches with the earlier study.[48] These winds were given as input to the MIKE21 HD to simulate hydrodynamics.

Fig. 4 to be inserted here

The West India Coastal Current (WICC), which is instigated due to the remote forcing, plays a major role in the AS circulation pattern[46]. The current flows like a jet in the vicinity of continental slope. The U and V velocity components of the currents obtained from the HD model were calculated for monthly averages while the tidal currents are being eliminated (See Fig. S10, Supporting Information). Figure S10 depicts that significant WICC flows equatorward along the continental slope during April to July. As a whole, the currents on the shelf are stronger and flow towards the southeast while the currents beyond the continental slope are weaker. We find that currents are stronger in the GoK (mouth to head); magnitudes of zonal components are smaller as tidal currents are removed by averaging. Tidal currents play a significant role in the circulation pattern off GoK, a macro-tidal regime, where tide range exceeds 7.0 m.

4.2. Trajectories from the PA model

Utilizing the above described winds and currents, PA model has been run for April, May, June and July in order to understand the forcing mechanism of TB transport during 15-17 July 2012 along the Tithal, Maroli, Umbergaon and Nargol beaches off south Gujarat.

4. 2. 1. April and May simulations

We have used a 2D model to calculate depth averaged currents, the entire water column was assumed as one layer. It has been assumed in the model that the tar ball particles are neutrally buoyant at the sea surface. Particles were released at 10 pre-determined locations on 2 April 2012. Only the particles P1 and P2 landed on to the coast between Tithal and Maroli, while the remaining 8 particles found their direction towards the south, without being washed on to the coast (Fig. 5a). Overall, the trajectories of the particles were towards the south. This is because, during April, winds are towards southeast (Fig. 4) and wind driven mean currents are towards southeast. Therefore, the resultant trajectories of the particles are towards the south-southeast.

Unlike in April, the trajectories during May have slightly deviated in an anticlockwise direction from south-southeast to southeast as shown in Fig. 5b. Since the particles P1 and P2 were near to the coast, they were the first to reach the coast as well. However, the locations where they were washed up are not our interest (no TB deposition). Subsequently, particles P3 and P4 reached Umbergaon and Nargol beaches, respectively, and regions around P3 and P4 may be the probable areas for the origin of the TB formation (it may be noted that there are a few BH wells in this region).

Fig. 5 to be inserted here

4. 2. 3. June and July simulations

The particle trajectories during June and July are entirely different from April and May trajectories. June simulation (Fig. 5c) shows that initially a few particles travelled towards east and directly reached the coast, while some of them turned towards northeast and then towards southeast (because of local tide effect) and finally landed on the coast. Particles P4, P5, P6 and P7 landed along the coastal stretch between Tithal and Nargol after 17, 18, 20 and 18 days of release, respectively. During June, under the influence of winds (south-westerly) and currents (towards southeast), the TB particles take a resultant direction towards east-northeast.

In July, the winds and currents are stronger than in June, while the direction is same. Particles P4, P5 and P6 precisely landed along the coastal stretch of Tithal, Maroli and Umbergaon. Rest of the particles - P1 and P2 landed far north of Tithal, and, P7, P8, P9 and P10 landed far south of the Nargol (region not of interest to us). Particles P4, P5 and P6 travelled for 15, 18 and 21 days to reach the coast (10^{th}, 13^{th} and 17^{th} July 2012, respectively), and this reasonably matches with the TB depositions that occurred during 15 -17 July 2012 along the beaches of Tithal, Maroli, Umbergaon and Nargol.

Based on the four months simulations, we can state that TB particles start moving from the region of origin during late May/June, and take a turn towards either east or northeast (particle trajectories during April to July shift in anticlockwise direction, Fig. 5) and reach the coast. During April to July, the mean surface current pattern in the domain is unchanging and it is in the southeast direction (See Fig. S10, Supporting Information). However, the winds change their direction: such as northwesterly in April, westerlies in May and southwesterlies in June and July. Therefore, the shift of trajectories from April to July must be primarily due to the influence of winds. The width of the continental shelf is maximum off GoK (250 km) and it decreases towards the south. This wider shelf (≈ 250 km) has less than 200 m depth, and is dominated by tidal currents and winds. A small influence of large-scale wind driven currents is also expected off GoK[49]. Therefore, the effect of open ocean currents is less in this region. Thus, winds, tidal currents played a major role together with the minor contribution of wind driven currents in the transportation of TBs to the south Gujarat coast during July 2012. BH is the leading offshore oil field in India, and is situated approximately 160 km west-northwest off Mumbai in the AS (Fig. 1b). It has more than 110 well platforms[50]. BH is divided into two blocks as BH North (BHN) and BH South (BHS). The crude oil produced from the BHN is pumped to Uran terminal through the MUT pipeline (See Fig. S11, Supporting Information). The particles at P3, P4, P5 and P6 locations are very near to the BHN platform.

The DRs of n-alkanes, PAHs, triterpanes, CSIA and PCA confirm that the source of the TBs is BH oil, and the transport model results confirm that the probable source locations are in the vicinity of BHN oil fields. Therefore, we can confidently state that the TBs deposited along the beaches of Tithal, Maroli, Umbergaon and Nargol during 15-17 July 2012 were of BHM origin. But, the question is, whether it is the operational spill in the BH oil fields or natural seepage from the BH basin is the culprit? A detailed research has to be conducted to answer this question, and we have just initiated this work.

Acknowledgements

We thank Dr. S.W.A Naqvi, Director, CSIR-NIO, Goa, India for his keen interest in this study. First author is grateful to CSIR, India for providing Senior Research Fellowship. We thank Gujarat Pollution Control Board for their kind support in sample collection. We also thank Dr. Srirama Krishna for his kind support to use GC-C-IRMS. Thanks are due to Dr. Aninda Muzumdar, for extending the Wet Lab facility. We also thank Dr. Veerasingam for his help in PCA. This is NIO contribution no. **xxxx.**

Supporting Information

Brief description of GC-MS is given in section SI. 2, and the consistency check performed for the GC-MS is given in Fig. S1 and data for the same is given in Table S1. Likewise, information on GC-IRMS and its calibration is given in SI. 3, and Table. S2 Calibration curves used for quantification of alkane, PAHs and hopanes are shown in Fig. S2. The comparison of HD model results with the measured currents is given in Fig. S3, presence of UCM in TB samples is shown in the Fig. S4, Fig. S5 and S6 are the distribution of PAH and hopane compounds. The Figs. S7 and S8 are the hopane chromatograms for the TBs and crude oil samples respectively and Table S3 is the compound name of the peaks shown in Figs S7 and S8. The monthly means of HD currents from Apr-July 2012 are illustrated in Fig. S10. Tables S4, S5, and S6 are the DRs of n-alkanes, PAHs, hopanes respectively. Locations of BH oil fields and pipelines are illustrated in Fig. S11.

References

(1). Zakaria, M.P., A. Horinouchi., S. Tsutsumi., H. Takada., S. Tanabe., and A. Ismail. Oil pollution in the straits of Malacca, Malaysia: Application of Molecular Markers for source identification. *Environmenal Science and Technology*, 2000, 34, 1189-1196.

(2). Zakaria, M. P., Tomoaki Okuda and Hideshige Takada. Polycyclic Aromatic Hydrocarbon (PAHs) and Hopanes in stranded Tar-balls on the coast of Peninsular Malaysia: Applications of Bimarkers for Identifying sources of oil pollution. *Marine Pollution Belletin*, **2001**, 42, 1357-1366.

(3). Wang Z; M. Fingas; C. Yang and Hollebone. Biomarker fingerprinting: Application limitation for correlation and source identification of oils and petroleum products. Prepr Pap-Am. Chem. Soc., Div. Fuel Chem. **2004**, 49 (1), 331

(4). Mulabagal, V., F. Yin., G.F. John., J.S. Hayworth., T.P. Clement. Chemical fingerprinting of petroleum biomarkers in Deepwater Horizon oil spill samples from Alabama shoreline. *Marine Pollution Bulletin*, **2013**, 70, 147–154.

(5). Katsoyiannis, A., Terzi, E., Cai, Q. On the use of PAH molecular diagnostic ratios in sewage sludge for the understanding of the PAH sources. Is this use appropriate? *Chemosphere*, **2007** 69, 1337–1339.

(6). Brandli, M., Bucheli, T.D., Kupper, T., Mayer, J., Stadelman, F.X., Taradellas, J. Fate of PCBs, PAHs and their source characteristic ratios during composting and digestion of source-separated organic waste in full-scale plants. *Environ. Pollut*, **2007** 148, 520–528.

(7). Chandru. K, MohamadPauziZakaria, Sofia Anita, AzadehShahbazi, MahyarSakari, PouryaShahpouryBahry, CheAbd Rahim Mohamed. Characterization of alkanes, hopanes, and polycyclic aromatic hydrocarbons (PAHs) in tar-balls collected from the East Coast of Peninsular Malaysia. *Marine Pollution Bulletin*, **2008**, 56, 950-962.

(8). Suneel, V., P. Vethamony., M. P. Zakaria., B. G. Naik., K. V. S. R. Prasad. Identification of sources of TBs deposited along the Goa coast, India, using fingerprinting techniques. *Mar. Pollut. Bull*. ., **2013a** 70; 2013; 81-89.

(9). Macko, S. A., Parker, P. L., Botello, A. V. Persistence of spilled oil in a Texas salt marsh. *Environ. Poll*, **1981**, 2, 119-28.

(10). Mansuy. L., R. Paul Philip and John Allen. Source Identification of oil spills based on the isotopic composition of individual components in weathered oil samples. *Environmental Science and Technology*, **1997**, 31, 3417-3425.

(11). Li. Y., Yongqiang Xiong., Wanying Yang., YueliangXie., Siyuan Li., Yongge Sun. Compound Specific stable carbon isotopic composition of petroleum hydrocarbons as a tool for tracing the source of oil spills. *Marine Pollution Bulletin*, **2009** 58, 114-117.

(12). Betti, M., F. Boison, M. Eriksson, I. Tolosa., E. Vasileva. Isotope analysis for marine environmental studies. *International Journal of Mass Spectrometry*, **2011**, 307(1-3), 192-199.

(13). Oulhote. Y; B. Le Bot; S. Deguen, P. Glorennec. Using and interpreting isotope data for source identification. *Trends in Analytical Chemistry*, **2011**, 30, 302-312.

(14). Wong. C. S., David R. Green, Water J. Creetney. Quantitative Tar and plastic waste distribution in the Pacific Ocean. *Nature*, **1973** Vol. 247 January 4, **1974**.

(15). Wong. C. S, David R. Green, Water J. Creetney (1976). Distribution and source of Tar on the Pacific Ocean. *Marine Pollution Bulletin*, Volume 7, Issue 6, June **1976**, Pages 102-106.

(16) Lebreton, L.C.M., S.D. Greer, J.C. Borrero. Numerical modelling of floating debris in the world's oceans. Marine Pollution Bulletin, **2012**, 64, 653–661.

(17) Lebreton, L.C.M., Borrero. Modeling the transport and accumulation floating debris generated by the 11 March 2011 Tohoku tsunami. Marine Pollution Bulletin, **2013,** 66, 53– 58.

(18) Martinez., E, Keitapu Maamaatuaiahutapu, Vincent Taillandier. Floating marine debris surface drift: Convergence and accumulation toward the South Pacific subtropical gyre. *Marine Pollution Bulletin*, **2009**, 58 1347-1355

(19). Suneel., V; Vethamony, P; Vinod Kumar, K; Babu, M. T; K. V. S. R. Prasad. Simulation of Trajectories of TB Transport to the Goa Coast. *Water Air Soil Pollut*, **2013b** 224:1538, DOI 10.1007/s11270-013-1538-9.

(20). Babu M.T., Vethamony P., Ehrlich Desa. Modelling tide-driven currents and residual eddies in the Gulf of Kachchh and their seasonal variability-A marine environmental planning perspective, *Ecological Modeling*, **2005**, 184, 299–312.

(21). Babu M.T., Kesava Das V., Vethamony P.,BOD–DO modeling and water quality analysis of a waste water outfall off Kochi west coast of India. *Environment International*, **2006**, 32, 165-173.

(22). Vethamony., P., Sudheesh K., Babu M.T., Jayakumar S., Manimurali R., Saran A.K., Sharma L.H., Rajan B., Srivastava M. Trajectory of an oil spill off Goa eastern Arabian Sea: field observations and simulations, *Envt Poll*, **2007a**, 148, 438 -444.

(23). Vethamony P., Babu M. T., Ramanamurty M. V., Saran A. K., Antony Joseph, Sudheesh K., Rupali S Padgaonkar., Jayakumar S.,Thermohaline structure of an inverse estuary – the Gulf of Kachchh: Measurements and model simulations, *Marine Pollution Bulletin*, **2007b**, 54, 697-707

(24). Grinson G., VethamonyP., SudheeshK., Babu M. T. Fish larval transport in a macro-tidal regime: Gulf of Kachchh, west coast of India, *Fisheries Research*, **2011**, 110, 160-169.

(25). Chetan A. G, Samiksha S.V., Grinson George., Aboobacker. V. M., Vethamony P., and Anil A. C., Numerical Simulations of barnacle larval dispersion coupled with field observations on larval abundance settlement and recruitment in a tropical monsoon influenced coastal marine environment, *Journal of Marine Systems,* **2012**, 94, 218-231.

(26). Rupali S.Patgaonkar, Vethamony P., Lokesh K. S., Babu M. T., Residence time of pollutants discharged in the Gulf of Kachchh northwestern Arabian Sea, *Marine pollution bulletin,* **2012** 64, 1659-1666.

(27). Samiksha S. V., Jahfer Sharif, P. Vethamony. Coastal circulation off Ratnagiri, west coast of India during monsoon seasons: a numerical model study. *Indian Journal of Geo-Marine Science*, **2014**, In press.

(28). Sindhu. B, I. Suresh, A. S. Unnikrishnan, N. V. Bhatkar, S. Neetu, G. S. Michael. Improved bathymetric datasets for the shallow water regions in the Indian Ocean. *Journal of Earth System Science*, **2007**, 166(3), 261-274.

(29). Wang, Z., M. Fingas, M. Landriault, L. Sigouin, B. Castle, D. Hostetter, D. Zhang, B. Spencer, 1998. Identification and linkage of TBs from the coast of Vancouver Island and Northern California using GC-MS and Isotopic techniques. Journal of High Resolution Chromatogram, 21, 383-395.

(30). Wang, Z., Fingas, M., Sergy, G. Study of 22-old Arrow oil samples using biomarker compounds by GC-MS. *Environmental Science and Technology*. **1994b** 28, 1733-1746.

(31) Dahlmann, G., Characteristic Features of different oil types in oil spill identification, Berichte des BSH, 2003, 31.

(32) Mahua Saha, Ayako Togo, Kaoruko Mizukawa, Michio Murakami, Hideshige Takada, Mohamad P. Zakaria, Nguyen H. Chiem, Bui Cach Tuyen, Maricar Prudente, Ruchaya Boonyatumanond, Santosh Kumar Sarkar, Badal Bhattacharya, Pravakar Mishra, Touch Seang Tana. Sources of sedimentary PAHs in tropical Asian waters: Differentiation between pyrogenic and petrogenic sources by alkyl homolog abundance. Marine pollution Bulletin, 2009, 58, 189-200

(33) Yim, U.H., Moonkoo Kim, Sung Yong Ha, Sunghwan Kim, and Won Joon Shim. Oil spill environmental forensics: the Hebei Spirit oil spill case. *Environmental Science and Technology,* **2012**, 46, 6431-7.

(34) Ananthy, R; Mohamad Pauzi Zakaria; Hafizan Juahir; Ahmad Zaharin Aris, Munirah Abdul Zali, Mohd Fadhil Kasim. Chemometric techniques in distribution, Characterisation and source apportionment of polycyclic aromatic hydrocarbons (PAHS) in aquaculture sediments in Malaysia. *Marine Pollution Bulletin*, **2013**, 69, 1- 2, 55-66.

(35) Boehm, P.D., D.S. Page, W.A. Burns, A.E. Bence, P.J. Mankiewicz, and J.S. Brown, Resolving the origin of the petrogenic hydrocarbon background in Prince William Sound, Alaska. *Environ. Sci. Technol*., 2001, **35**, 471–479.

(36) Page, D. S., Boehm, P. D., Douglas, G. S. and Bence, A. E. Identification of hydrocarbon sources in the benthic sediments of Prince William Sound and the Gulf of Alaska following the *Exxon Valdez* Oil Spill. In Exxon Valdez Oil Spill." Fate and Effects in Alaskan Waters, ASTMSTP 1219, eds P. G. Wells, J. N. Butler and J. S. Hughes, 1995, 41-83. American Society for Testing and Materials, Philadelphia, PA.

(37) Wang, Z.D., M. Fingas, and G. Sergy, Chemical characterization of crude oil residues from an arctic beach by GC-MS and GC-FID. *Environ. Sci. Technol.*, **1995b**, 29, 2622– 2631.

(38) Peters, K. E., C. Walters., J. M. Moldowan. The Biomarker guide, Volume 2, 2005, Cambridge University press.

(39) Sosrowidjojo, I.B., Alexander, R. and Kagi, P., 1994. The biomarker composition of some crude oils from Sumatra. Organic Geochemistry 21, 303-312.

(40) Barakat, A. O; Alaa R. Mostafa, Jurgen Rullkotter and Abdel Rahman Hegazi. Application of a Multimolecular Marker Approach to Fingerprint Petroleum Pollution in the Marine Environment. *Marine Pollution Bulletin*, **1999**, 38, 7 535-544.

(41). Volkman, J. K, A. T. Revil and A. P. Murray. Application of biomarkers for identifying sources of natural and pollutant hydrocarbons in aquatic environments, In: R. P. Eganhouse (ed), *Molecular Markers in Environmental Geochemistry*, American Chemical Society, Washington DC, **1997**, 83-89.

(42). Anita, S. Distribution and source of oil pollution using TBs as indicator in northeast Sumatra, Indonesia via fingerprinting techniques. *PhD. Dissertation*, University Putra Malaysia, **2009**.

(43) Macko, S. A., Patrick, L. Parker. Strable Nitrogen and Carbon Isotope Ratios of Beach tars on South texas barrier Islands. Marine Environmental Research, **1983** 10, 93-103.

(44) Murray, A.P., R.E. Summons, C.J. Boreham, and L.M. Dowling. Biomarker and n-alkane isotope profiles for Tertiary oils: Relationship to source rock depositional setting, Organic Geochemistry, **1994**, 22, 521–542.

(45) Hunt J. M, R. Paul Philp, Keith A. Kvenvolden. Early developments in petroleum geochemistry. Organic Geochemistry, 2002, 33, 1025-1052

(46) Shankar D., Vinayachandran P. N. and Unnikrishnan A. S. The monsoon currents in the north Indian Ocean, *Prog Oceanogr*, **2002**, 52, 63– 120.

(47) Sontro T. S. D, Ira Leifer, Bruce P. Luyendyk, Bernardo R. Broitman. Beach tar accumulation, transportation mechanisms, and sources of variability at coal oil point, California. *Marine Pollution Bulletin*, **2007**, 54, 1461-1471.

(48). Shetye S. R., Gouveia A.D., Shenoi S.S.C., Micheal G.S., Sundar D., Almeida A.M, Santanam K. The coastal current off western India during the northeast monsoon, *Deap-Sea Research*, **1991**, 38, , 1517-1529.

(49). Unnikrishnan A. S,, S. R. Shetye and G. S. Michael. Tidal propagation in the Gulf of Khambhat, Bomabay High, and surrounding areas. Proc. Indian Acad. Sci. *Earth Planet Sci*, **1999**, 108, 3, 155-177.

(50). Mitra, N.K., SPE, P.K. Dileep, SPE, and Adesh Kumar. Revival of Mumbai High North - A Case Study. SPE, Oil and Natural Gas Corporation Ltd., India. SPE Indian Oil and Gas Technical Conference and Exhibition, 4-6 March, Mumbai, India. *Society of petroleum Engineers*, **2008**, ISBN 978-1-55563-192-5, document ID 113699-MS.

Figures

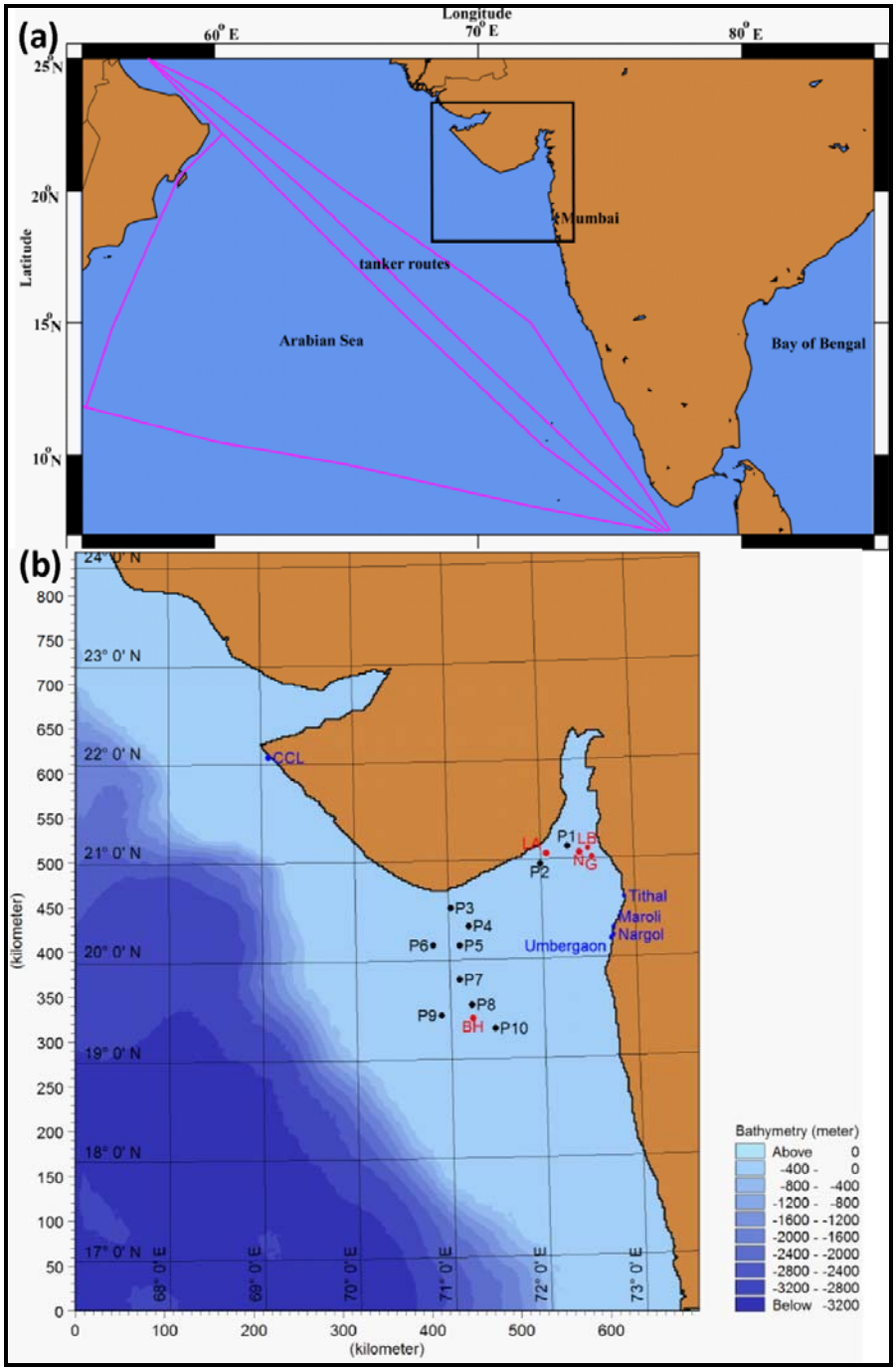

Fig.1. (a) International oil tanker routes in the Arabian Sea; (b) model domain indicated in Fig. (a); BH is Bombay High platform; LA, LB and G are oil rig locations belonging to Cairn Energy (Pvt) Ltd; N is the location of NIKO (Pvt) Ltd; P1-P10 are locations, from where particles (TBs) are released. CCL is the location at which modeled currents are compared with observed currents.

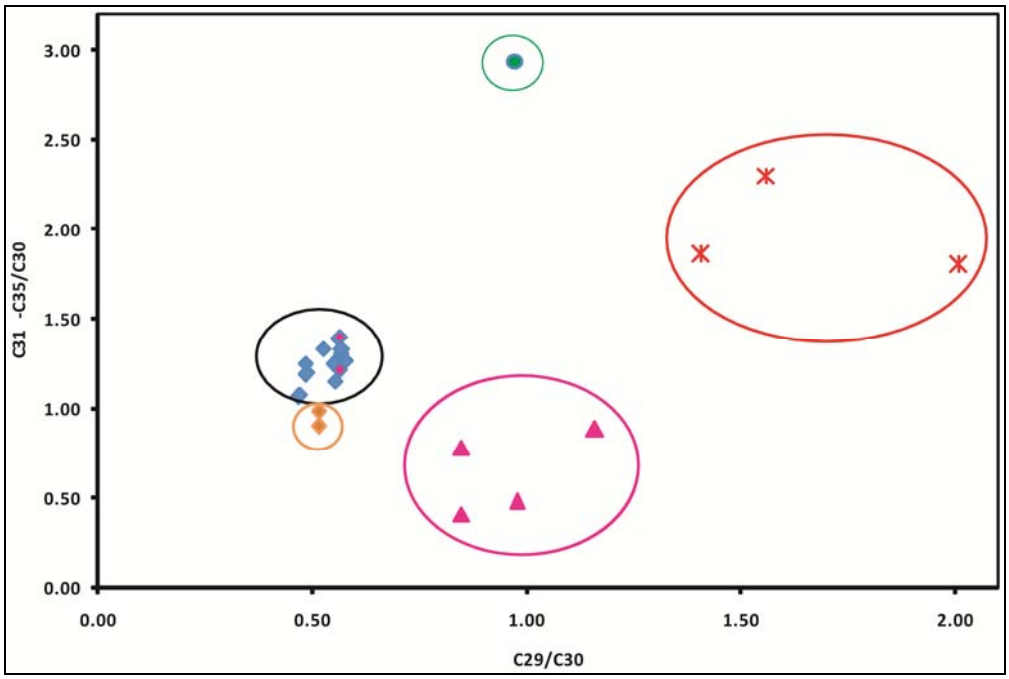

Fig. 2. Cross plot of homohopane index. The red circle represents MECO, pink-SEACO, orange-CRN and NIK, green-MSC crude oil, black circle contains TBs (blue color) and BHH (pink color top) and BHM (pink color down).

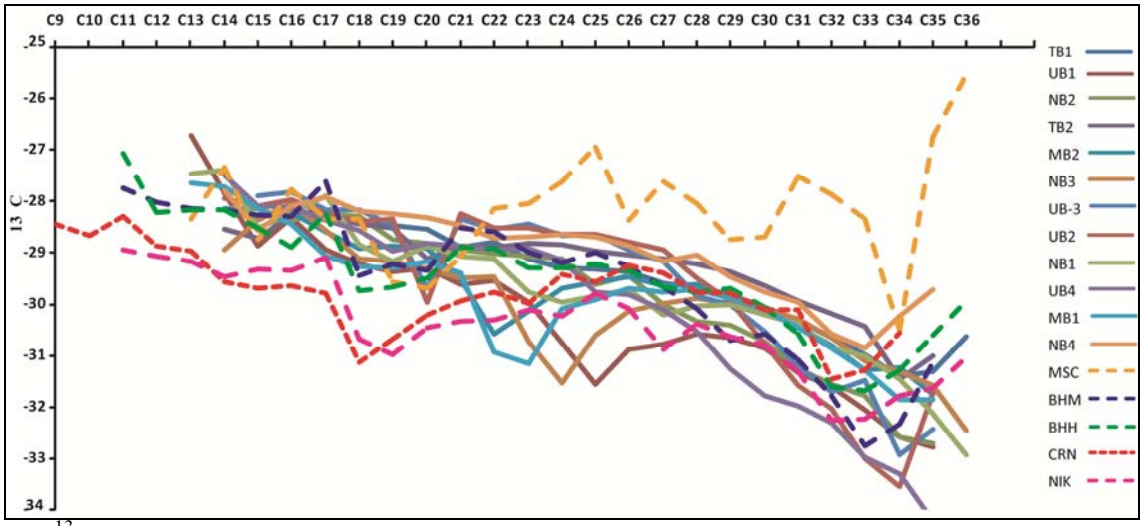

Fig. 3. $\delta^{13}C$ ratios for TBs and crude oil. Dash lines are for crude oil (red -CRN; pink - NI; blue- BHM, green - BHH, and dark yello - MSC crude oils; Remaining lines for TB sample**s.**

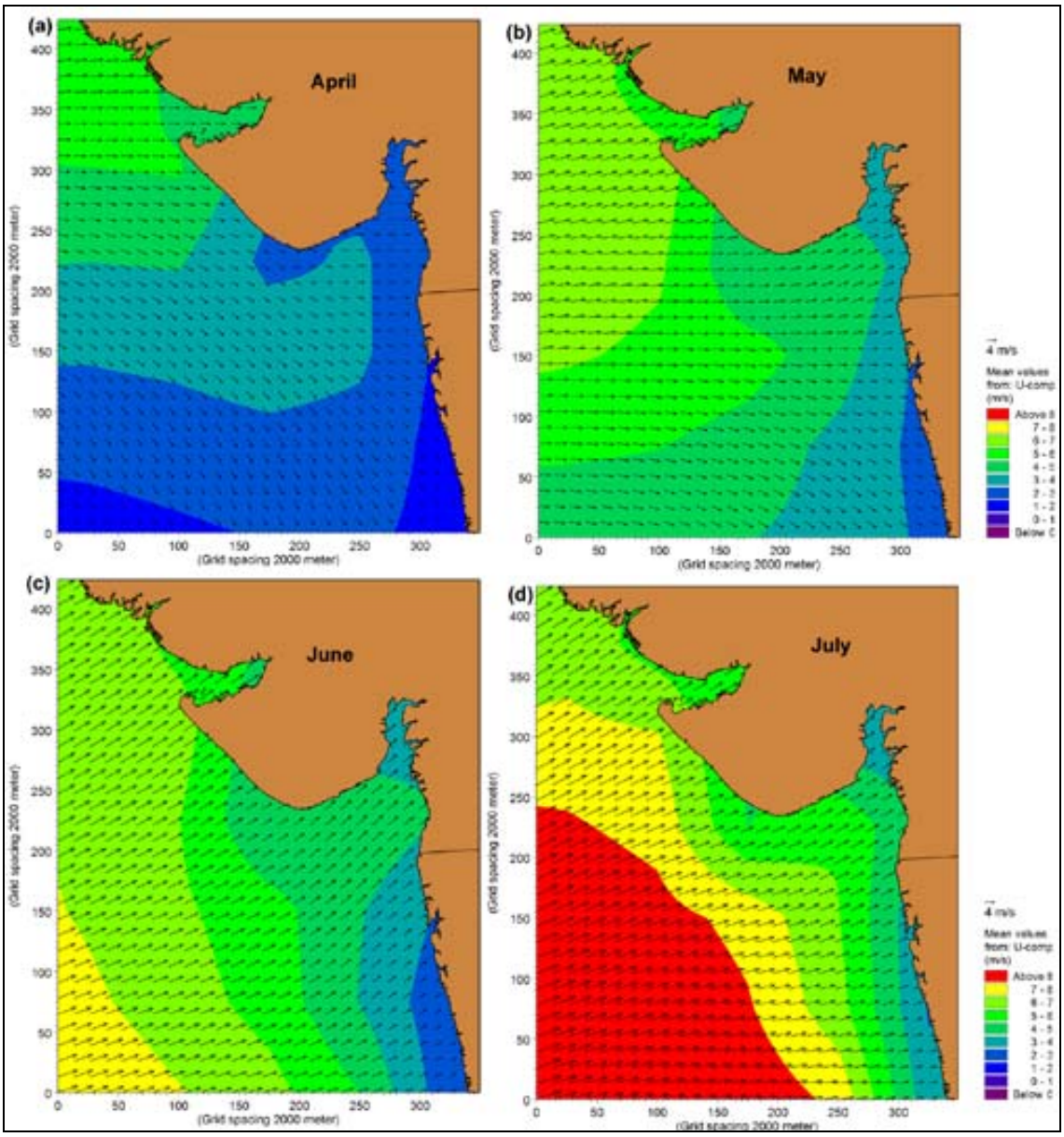

Fig. 4. Typical monthly average of wind fields of: (a) April, (b) May, (c) June and (d) July.

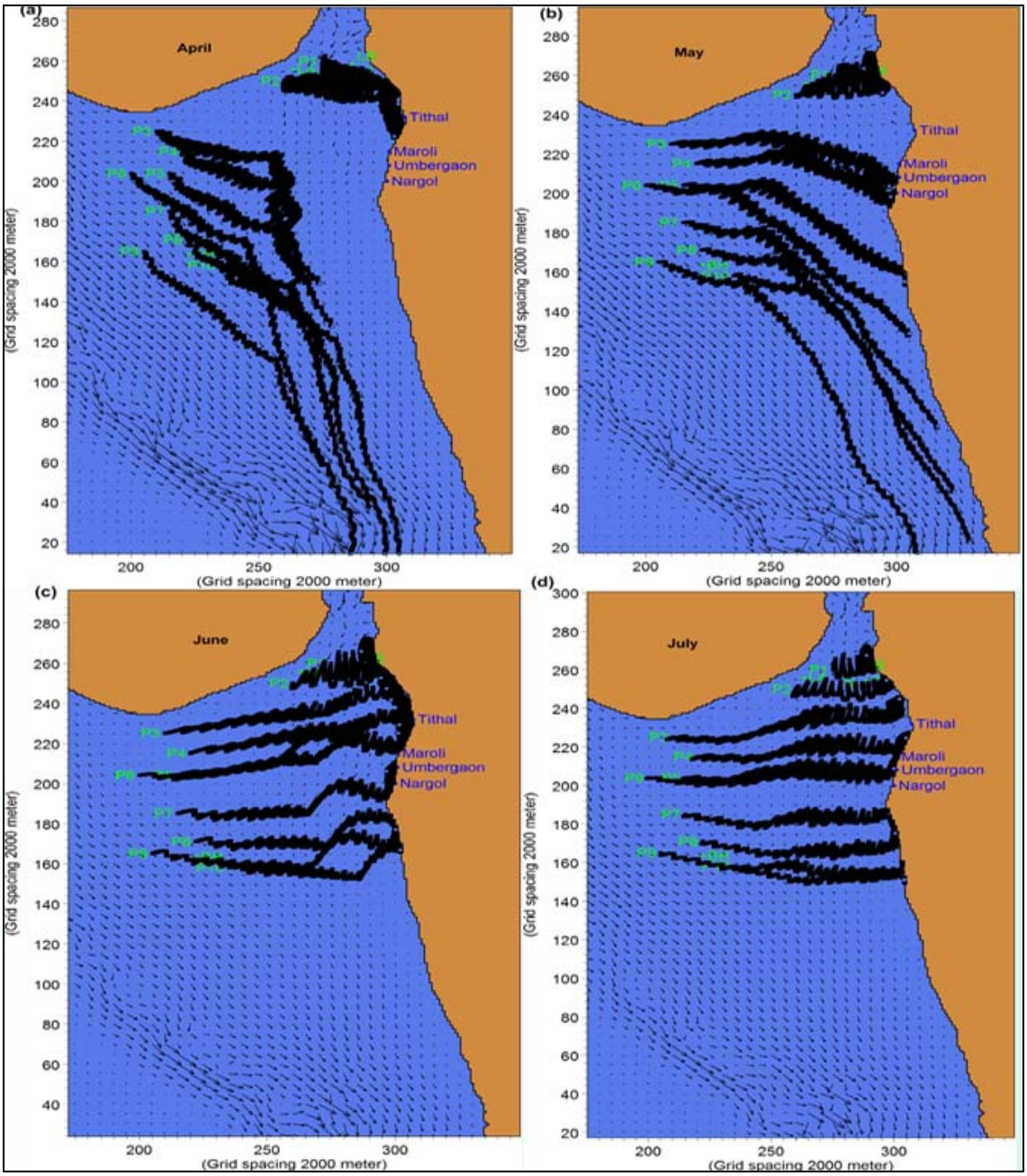

Fig. 5. Trajectories of TBs obtained from the PA model for (a) April, (b) May, (c) June and (d) July.

Supporting Information

SI. 1. Analytical procedure

Crude oil and tar ball samples were weighed precisely (130 mg) and dissolved in 50 ml of n-hexane; from this solution,10 ml of solution (containing the raw sample weight of 26 mg) was taken and transferred to 5% H_2O deactivated silica gel column (1cm i.dx 9cm). Hydrocarbons ranging from alkanes to PAH were eluted with 25 mL of DCM/hexane (1:3 v/v); 5 gm of activated copper was added to the collected elute and allowed to stand overnight to react with sulphur. Then the copper was removed and the sample was subject to roto-evaporation to decrease the volume to 2 mL. The sample was then transferred to the fully activated silica gel column (0.47cm i.d x 18 cm). Two fractions were eluted. The first fraction (F1) was eluted with 10 mL of hexane containing the aliphatic and alicyclic hydrocarbons (Aliphatic hydrocarbon fraction). The second fraction (F2) was eluted with 20 mL of hexane/DCM (3:1, v/v) containing the higher molecular weight PAHs (Aromatic Fraction). These two fractions were evaporated to dryness under the nitrogen blow down and rinsed with DCM HPLC grade and transferred to 1.5 mL ampoule, and added with 200-µL isooctane for further GC-MS analysis. F1 is used for analysis of the total saturates and isoprenoids, and biomarker compounds and F2 for alkylated PAH homologues and other EPA priority parent PAHs. However, F2 data lack authentication with authentic standards and will be used in future publication after verification

SI. 2. GC-MS

Using helium as the carrier gas, a fused silica capillary column RXi-5 of RESTEK 30m × 0.25mm id (0.25 µm film thickness) was used in GC-MS. The injector and detector temperatures were set to 280^{o}C and 220^{o}C, respectively. The oven temperature program was: 1 min hold at 40^{o}C; ramp to 10^{o}C at 140^{o}C/min; and ramp to 320^{o}C at 6^{o}C/min and finally a 15 min hold at 320^{o}C. Analyses for EPA-16PAH, were performed using the same GC-MS with a fused silica capillary column RXi-5 of RESTEK 60m × 0.25mm id (0.25 µm film thickness). The injector and detector temperatures were set to 220^{o}C. The oven temperature program was 2 min hold at 70^{o}C; ramp to 30^{o}C at 150^{o}C/min; ramp to 4^{o}C at 310^{o}C/min and finally a 0.33 min hold at 310^{o}C. The consistency of the GC-MS was checked with 5 runs of n-alkane standard (C_8-C_{40} n-alkane). All the runs are consistent with each other (Fig. S1 and Table. S1)

The n-alkanes, pristane and phytane were identified by comparing the retention time with authentic standards within a range of +/- 0.01 min. The mass spectra was identified based on the authentic standards and National Institute of Standards and Technology (NIST) spectral reference library, and finally, the particular ratios of several relatively abundant ions. The mode of analysis was electron ionization (EI) scan and SIM mode with 70 eV. The pentacyclic tri-terpenoids present in the aliphatic hydrocarbon fraction were determined with electron ionization (EI) SIM mode by monitoring m/z 191. The 17β(H)21α(H)-hopane ($C_{30}17\beta\alpha$) and 17α(H),22,29,30-trisnorhopane(Tm) were identified by comparing retention time with authentic standards. Other hopanes were confirmed by comparing their retention time with the authentic hopane standards $C_{30}17\beta\alpha$ and Tm, mass spectra from published data. The quantification for n-alkane, PAHs and hopanes were done utilizing the calibration standards of various concentrations. The initial calibration is done at the following five levels (three for hopanes): 5, 10, 15, 25, 30 ppm (µg/ml) for alkanes; 1.5, 3, 4, 6.5 and 10 ppm (µg/ml) for EPA 16 PAH; 2, 10, 20 ppm (µg/ml) for $C_{30}17\alpha\beta$ hopane and 2, 8, 20 ppm for Tm hopane. Levels of calibration standards were selected based on the concentration ranges of molecular markers of samples from the preliminary analysis and detection limits. Response factors and linear curves were generated using inbuilt facilities of the software accompanied with QP 2010 GC-MS of Shimadzu by (CLASS-5000 Ver-2). Similar calibration curves were also generated for SIS and IIS. A set of calibration curves for calibration standards of few n-alkane, PAH and hopane, SIS and IIS, are shown in Fig. S2. Reproducibility of the whole analytical procedure was checked through triplicate analysis of a few crude oil samples. Relative standard deviation of the individual alkanes and hopane standards concentration were less than 10% and 15%, respectively (Table S1).

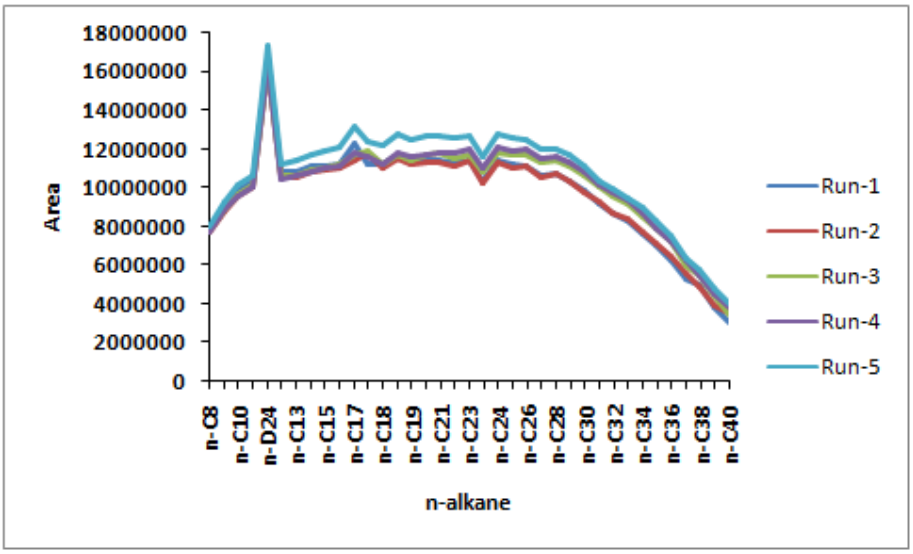

Fig. S1. Consistent test performed for GC-MS by n-alkane standard runs

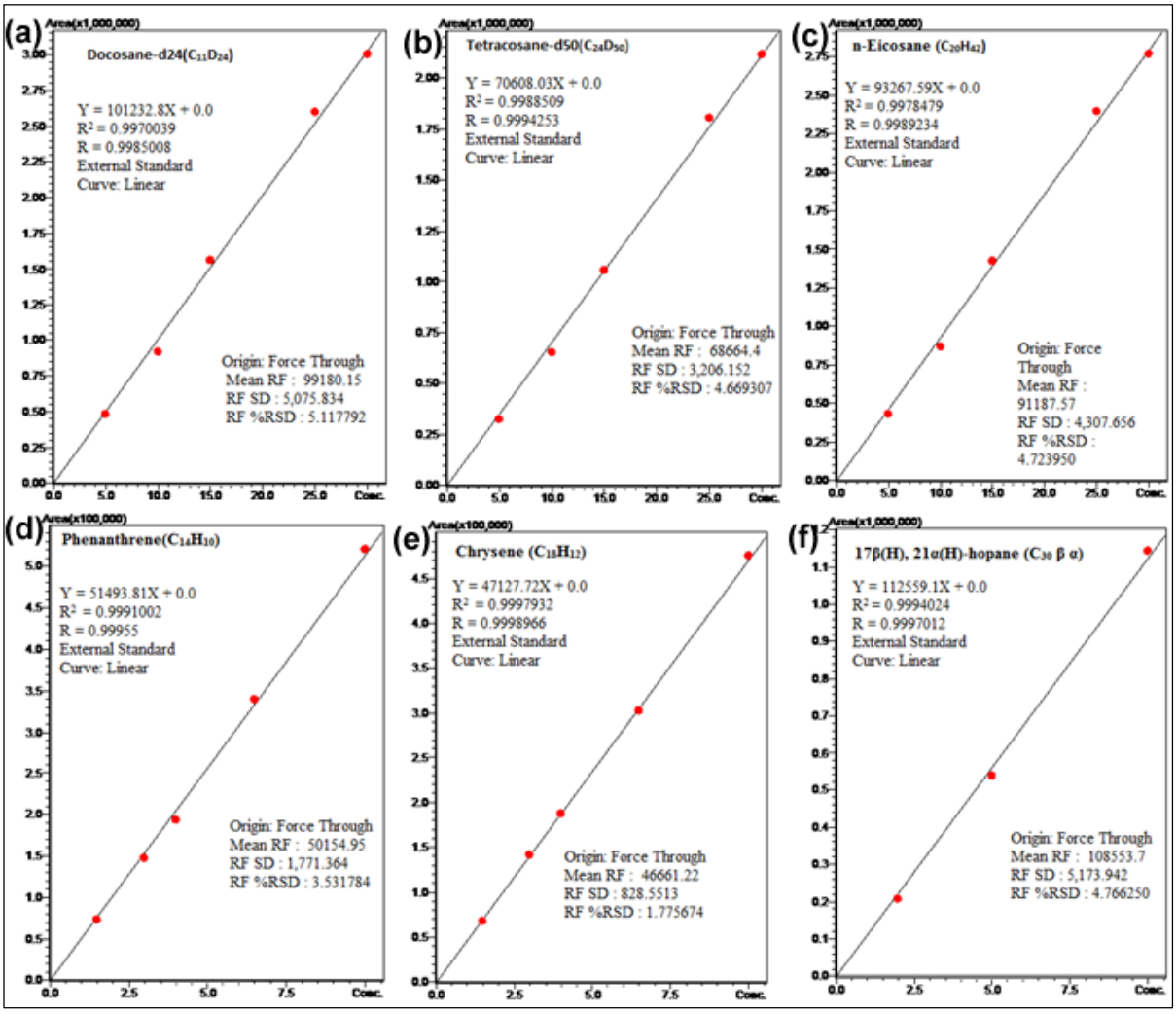

Fig. S2. Calibration curves for n-alkane, PAH and Hopane compounds

Table S1. Areas of the GC-MS consistent test performed to n-alkane standards

		1-Run	2-Run	3-Run	4-Run	5-Run			
s.n	Comp.	Area	Area	Area	Area	Area	Average	STDEV	RSD
1	n-C8	7869385	7725869	7811341	7731894	7973690	7822436	103353.9	1.32
2	n-C9	8984261	8800230	8860585	8867552	9252841	8953094	180320.8	2.01
3	n-C10	9815240	9571044	9660357	9543846	10098173	9737732	227644.9	2.34
4	n-C11	10335948	10063431	10157069	10072936	10601325	10246142	226681.3	2.21
5	n-D24	16683147	16202977	16310327	16267735	17321798	16557197	466552	2.82
6	n-C12	10814411	10503023	10670711	10443691	11226976	10731762	312690.5	2.91
7	n-C13	10792424	10540700	10632033	10592476	11371399	10785806	340610.7	3.16
8	n-C14	11066612	10855590	10892047	10834907	11740109	11077853	381332.2	3.44
9	n-C15	11088089	10890992	11008461	10968114	11937182	11178568	430002.6	3.85
10	n-C16	11200541	11030957	11177516	11072812	12083301	11313025	436349.9	3.86
11	n-C17	12281324	11413637	11691019	11800000	13127503	12062697	672689.1	5.58
12	Pristane	11180101	11766044	11847229	11586160	12361474	11748202	428725.9	3.65
13	n-C18	11177302	11032032	11215548	11248173	12210935	11376798	473548.5	4.16
14	Phytane	11680446	11541317	11730944	11792621	12732790	11895624	477077.3	4.01
15	n-C19	11395486	11221752	11423073	11602671	12503984	11629393	507216.7	4.36
16	n-C20	11423479	11289803	11651924	11717297	12666834	11749867	540756.4	4.60
17	n-C21	11447330	11316553	11747213	11772161	12687125	11794076	535834.4	4.54
18	n-C22	11277547	11121398	11524622	11788245	12596359	11661634	580493.6	4.98
19	n-C23	11403432	11361542	11698879	12003684	12705142	11834536	551031.5	4.66
20	n-D50	10338984	10268115	10789323	10997416	11595200	10797808	540102.6	5.00
21	n-C24	11396689	11283924	11787959	12048094	12762940	11855921	592095.3	4.99
22	n-C25	11216071	11013479	11684150	11875176	12559615	11669698	606379.2	5.20
23	n-C26	11126112	11088582	11686882	12001044	12500848	11680694	598638.6	5.13
24	n-C27	10654922	10548527	11268072	11472222	12009424	11190633	603115.7	5.39
25	n-C28	10703069	10747803	11435317	11562485	12005882	11290911	558192.1	4.94
26	n-C29	10311366	10326203	11102240	11293164	11685976	10943790	608149.3	5.56
27	n-C30	9799155	9785404	10629441	10831335	11065359	10422139	595333.5	5.71
28	n-C31	9209083	9233097	9995516	10089961	10291463	9763824	506916.7	5.19
29	n-C32	8679083	8711616	9553346	9704330	9932948	9316265	582816.7	6.26
30	n-C33	8252935	8395318	9202674	9396193	9499049	8949234	582656.8	6.51
31	n-C34	7628747	7719948	8516336	8716605	8985654	8313458	607580.8	7.31
32	n-C35	6990364	7114901	7876579	7892810	8246048	7624140	543984.1	7.14
33	n-C36	6243633	6458287	7233057	7202071	7536681	6934746	553946.8	7.99
34	n-C37	5248691	5551666	5988792	6217702	6308541	5863078	451233.9	7.70
35	n-C38	4954786	4923142	5493781	5428058	5732671	5306488	354308.6	6.68
36	n-C39	3851926	3925495	4409327	4494442	4767678	4289774	390187.2	9.10
37	n-C40	3024707	3520942	3444738	3839459	3966482	3559266	369009.4	10.37

SI. 3. GC-IRMS

The GC was equipped with a HP-5 MS column (30m X 0.25mm inner diameter with 0.25 μm film thickness). The oven temperature program was: 1 min hold at 70^{o}C; ramp to 140^{o}C at 10^{o}C/min; again ramp to 300^{o}C at 6^{o}C /min and finally a 30 min hold at 310^{o}C with helium as the carrier gas. Initially, instrument was calibrated using the A5-mix NIST standards. The reproducibility of the results were checked with triplicate analysis of A5 mix standards contain 15 n-alkane compounds and C3 mix standards contain 5 n-alkane compounds. The standard deviations are in the range of 0.18-0.26(‰) for A5 and 0.05-0.06 for C3 standards (Table. S2). Results were reported in the standard delta notation as per mil (‰) deviations from the VPDB (Vienna ***pee Dee belemnite***).

Table S2. $\delta^{13}C$ values in per mill (‰) observed for A5 mix and C3 Mix NIST Standard.

A5 mix							
Abbrv.	**Actual**	**Run-1**	**Offset**	**Run-2**	**Offset**	**Run-3**	**Offset**
n-C_{16}	-26.15	-26.65	0.50	-26.57	0.42	-26.74	0.59
n-C_{17}	-31.88	-32.35	0.47	-32.13	0.25	-32.34	0.46
n-C_{18}	-31.11	-31.58	0.47	-31.42	0.31	-31.54	0.43
n-C_{19}	-31.99	-32.50	0.51	-32.29	0.30	-32.43	0.44
n-C_{20}	-32.35	-32.83	0.48	-32.67	0.32	-32.74	0.39
n-C_{21}	-29.1	-29.60	0.50	-29.40	0.30	-29.54	0.44
n-C_{22}	-32.87	-33.35	0.48	-33.10	0.23	-33.27	0.40
n-C_{23}	-31.77	-32.40	0.63	-32.12	0.35	-32.13	0.36
n-C_{24}	-33.34	-34.12	0.78	-33.85	0.51	-33.92	0.58
n-C_{25}	-28.48	-29.37	0.89	-29.25	0.77	-29.22	0.74
n-C_{26}	-32.94	-33.81	0.87	-33.74	0.80	-33.66	0.72
n-C_{27}	-30.49	-31.48	0.99	-31.29	0.80	-31.38	0.89
n-C_{28}	-32.21	-33.13	0.92	-33.12	0.91	-33.03	0.82
n-C_{29}	-31.08	-31.93	0.85	-31.94	0.86	-31.85	0.77
n-C_{30}	-29.84	-30.54	0.70	-30.71	0.87	-30.55	0.71
STDEV			**0.19**		**0.26**		**0.18**
AVG			**0.67**		**0.53**		**0.58**
C3 mix							
n-C_{17}	-31.16	-31.79	0.63	-31.62	0.46	-31.57	0.41
n-C_{19}	-33.17	-33.72	0.55	-33.68	0.51	-33.60	0.43
n-C_{21}	-29.1	-29.72	0.62	-29.64	0.54	-29.54	0.44
n-C_{23}	-31.77	-32.40	0.63	-32.21	0.44	-32.18	0.41
n-C_{25}	-28.48	-29.18	0.7	-29.02	0.55	-29.04	0.56
STDEV			**0.05**		**0.05**		**0.06**
AVG			**0.63**		**0.5**		**0.45**

SI. 4. HD Model and PCA

(a). HD model description

A cartesian coordinate system is used in the model with a grid size of 2000m x 2000m. HD is forced by ECMWF (European Centre for Medium-Range Weather Forecasts) reanalysis winds of 0.75^{o}x0.75^{o} resolution (http://data-portal.ecmwf.int/data/d/interim_daily/) and water levels predicted for open boundaries from Global Tidal Model (inbuilt in MIKE ZERO). Hydrodynamic model is validated with the currents measured off Dwaraka during December 2007. We find good agreement between modelled and observed currents (Fig. S3).

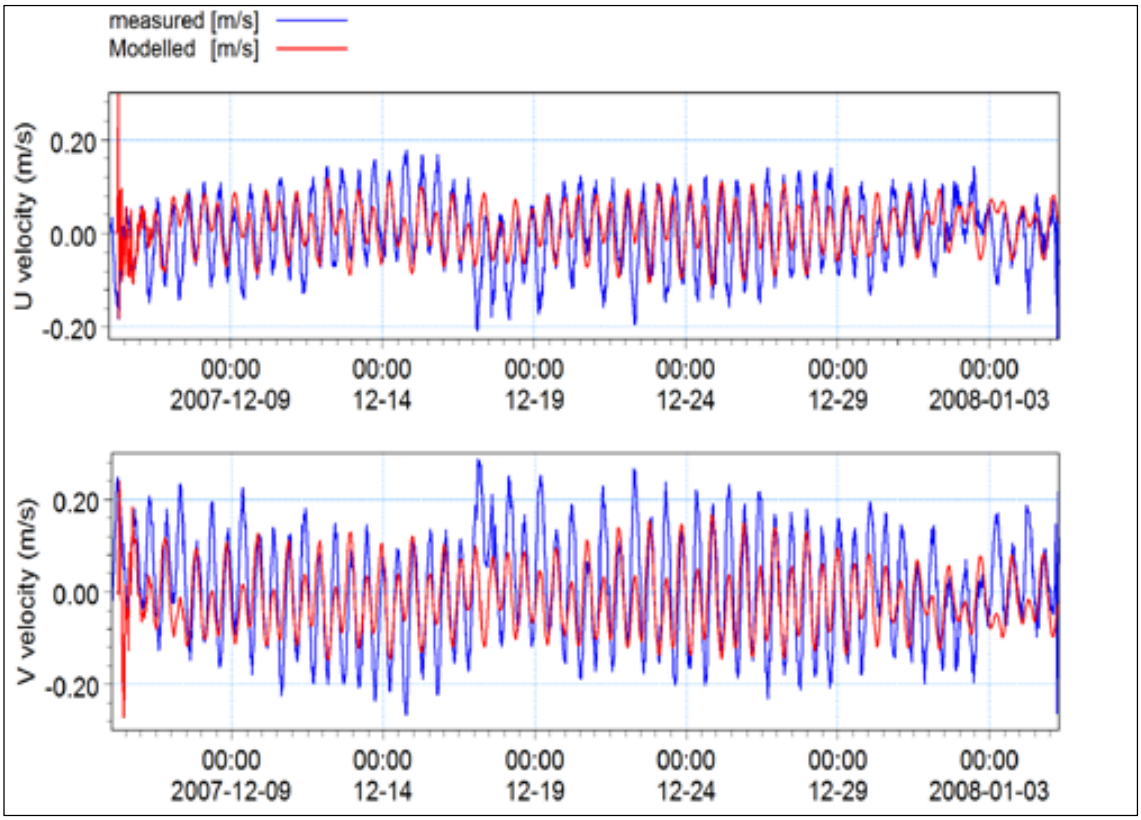

Fig. S3. Comparison of modeled currents with measured currents off Dwaraka (Dec. 2007 to Jan 2008).

These modelled currents were given as input to PA model. PA model is based on the Lagrangian random walk technique. We introduced numerically neutrally buoyant particles (follows the flow without being settled) in the flow field at 10 locations in the PA model domain -P1(72.288, 21.127), P2(71.994, 20.955), P3(71.023, 20.527), P4(71.210, 20.342), P5(71.109, 20.145), P6(70.823,

20.151), P7(71.101, 19.802), P8(71.229, 19.547), P9(70.902, 19.445), P10(71.470, 19.306). The model was forced with currents generated from the HD model and ECMWF surface winds.

(b). Principle Component Analysis (PCA)

PCA is a multivariate statistical tool that is widely used in the interpretive of oil spill fingerprinting**.** The PCA transforms the data into principal components. Samples of similar chemical compositions are clustered together and separate the samples that are chemically different. Therefore it helps in source identification, especially not to misidentify.

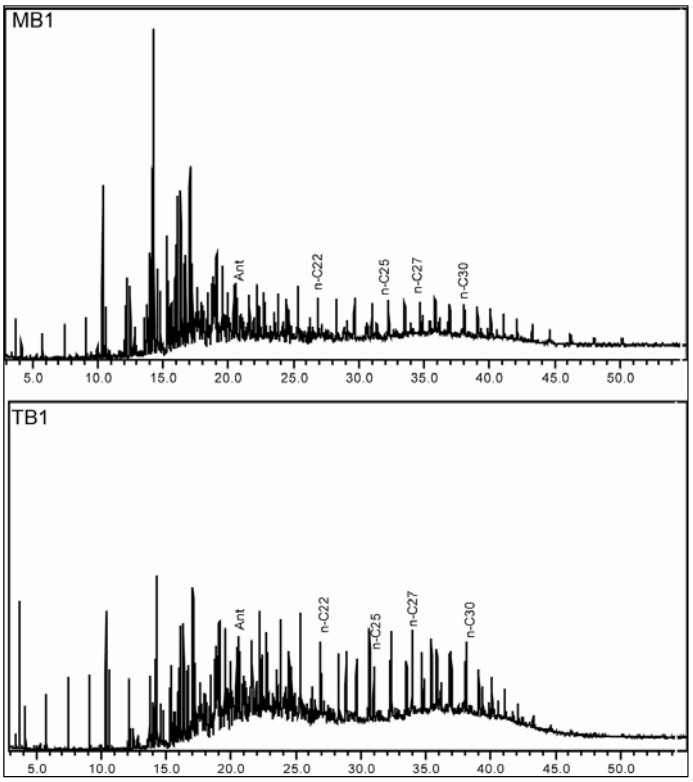

Fig. S4. Illustrates the presence of Unresolved Complex Mixture in, randomly selected two tar ball samples MB1 and TB1 are run in the scan mode (mixture of F1 and F2)

Table. S4. n-alkanes DRs

Sample	Pr/ph	C_{17}/Pr	C_{18}/Ph	C_{17}/C_{18}	CPI	L/H	WI	ΣAlkanes
UB-1	4.37	0.75	3.56	0.92	1.19	0.79	0.10	103370.32
UB-3	4.77	0.87	4.38	0.95	1.19	1.07	0.16	105569.10
UB-4	4.44	0.90	4.27	0.94	1.19	1.04	0.13	123762.82
NB-1	4.58	0.89	4.30	0.95	1.19	0.82	0.12	90238.47
NB-2	4.52	0.91	4.30	0.95	1.19	0.80	0.13	98160.00
NB-3	4.63	0.84	4.11	0.95	1.18	0.80	0.11	74902.48
NB-4	4.43	0.84	3.93	0.95	1.19	0.78	0.09	68119.68
MB-1	4.63	0.88	4.42	0.92	1.18	0.87	0.11	96723.49
MB-2	4.59	0.83	4.15	0.92	1.19	0.99	0.12	105609.63
TB-1	4.56	0.85	4.25	0.91	1.19	1.25	0.08	105902.72
TB-2	4.22	0.68	3.39	0.85	1.19	0.69	0.04	185010.65
MSC	0.73	5.97	4.10	1.07	1.10	3.03	1.07	12974.55
BHM	4.99	0.96	4.81	1.00	1.09	1.53	0.26	154685.71
BHH	6.03	0.94	5.67	1.00	1.11	1.37	0.21	182585.77
NIK	5.56	1.78	9.85	1.00	1.10	1.77	0.29	424482.09
CRN	6.38	1.71	9.83	1.11	1.10	3.10	0.73	190197.73

Pr/ Ph: ratio of Pristane to Phytane, C_{17}/Pr = ratio of n-C_{17} to Pristane; C_{18}/Ph = ratio of n-C_{18} to Phytane, CPI: Carbon Preference Index, L/H: ratio of sum of n-C_{16} to n-C_{26} relative to n-C_{27} to n-C_{36}.

$$\text{CPI}= \frac{1}{2} \text{x} \left[\left(\frac{C_{25}+C_{27}+C_{29}+C_{31}+C_{33}}{C_{26}+C_{28}+C_{30}+C_{32}+C_{34}} \right) + \left(\frac{C_{25}+C_{27}+C_{29}+C_{31}+C_{33}}{C_{24}+C_{26}+C_{28}+C_{30}+C_{32}} \right) \right] \quad \text{WI} = \left(\frac{C_{8}+C_{10}+C_{12}+C_{14}}{C_{22}+C_{24}+C_{26}+C_{28}} \right)$$

Table. S5. EPA priority PAHs DRs

Sample	Ant/(Ant+Phe)	Fth/(Fth+pyr)	BaA/(BaA+Chr)	Phe/Ant	Fth/pyr	∑MP/P	L/H
UB-1	0.96	0.34	0.69	0.04	0.52	65.22	6.21
UB-2	0.96	0.34	0.67	0.04	0.52	65.59	7.36
UB-3	0.97	0.35	0.66	0.04	0.53	66.83	8.35
UB-4	0.98	0.29	0.68	0.02	0.41	105.07	8.58
NB-1	0.96	0.34	0.67	0.04	0.52	63.09	7.99
NB-2	0.97	0.34	0.66	0.04	0.52	64.01	8.22
NB-3	0.96	0.34	0.66	0.04	0.51	62.08	7.14
NB-4	0.98	0.30	0.69	0.02	0.43	128.54	8.75
MB-1	0.97	0.34	0.67	0.03	0.52	71.04	7.97
MB-2	0.98	0.29	0.68	0.02	0.42	117.71	8.07
TB-1	0.97	0.30	0.69	0.03	0.43	44.46	6.23
TB-2	0.98	0.30	0.72	0.02	0.42	152.18	4.37
MSC	0.82	0.09	0.57	0.21	0.10	6.18	5.96
BHH	0.98	0.28	0.68	0.02	0.39	111.22	5.31
BHM	0.97	0.28	0.68	0.03	0.39	100.48	4.77
CRN	0.89	0.53	0.42	0.13	1.12	31.64	4.10
NIK	0.93	0.53	0.37	0.07	1.11	38.51	3.07
STD	0.007	0.024	0.017	0.008	0.052		

STD: standard deviation

Phe/Ant: Ratio of Phenanthrene to Anthracene,
Ant/Ant+phe: Ratio of Anthracene to sum of (Anthrace+Phenanthrene),
Fth/pyr: Ratio of Fluoranthene to Pyrene
Fth/Fth+Pyr: Ratio of Fluoranthene to sum of (Fluoranthene+Pyrene)
BaA/BaA+Chr: Ratio of Benza(a)anthracene to sum of (Benza(a)anthracene+Chrysene)
∑MP/P: Ratio of sum of 3-Methyl-Phenanthrene, 2-Methyl-Phenanthrene, 9-Methyl-Phenanthrene, 1-Methyl-Phenanthrene to Phenanthrene
L/H: The ratio of sum of low molecular weight components (Naphtalene, Acenaphtylene, Acenaphtene, Fluorene, Anthracene, Phenanthrene, , Fluoranthene, Pyrene) to high molecular weight components(Chrysene, Benzo(a)anthracene, Benzo(b)fluoranthene,Benzo(k)fluoranthene, Benzo(a)pyrene, Benzo(g,h,l) perylene, benzo(a,h)anthracene, Indeno(1,2,3- c,d)pyrene (InP))

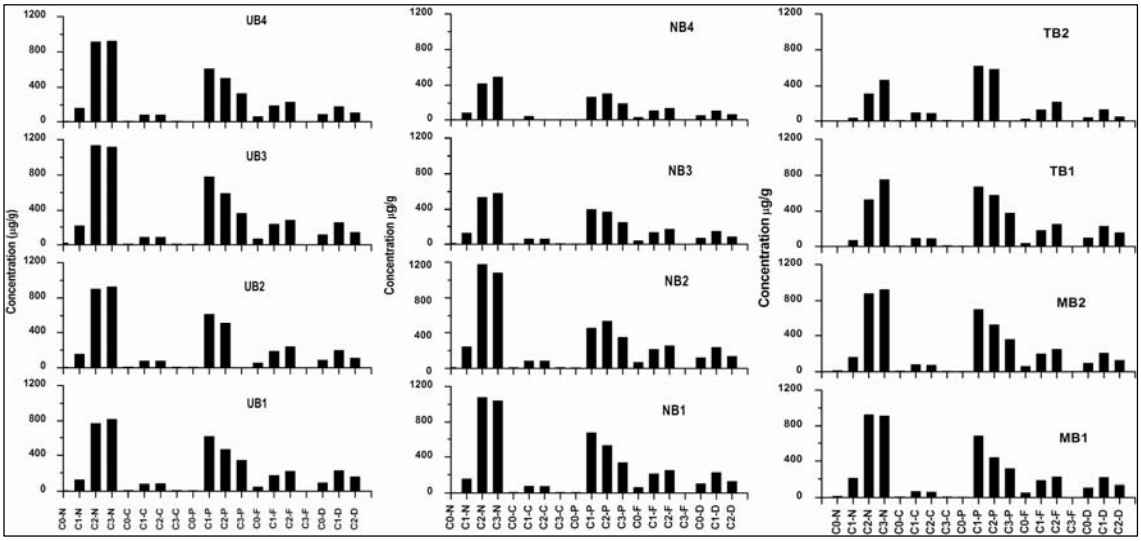

Fig. S5. Alkylated PAH in all tar ball samples

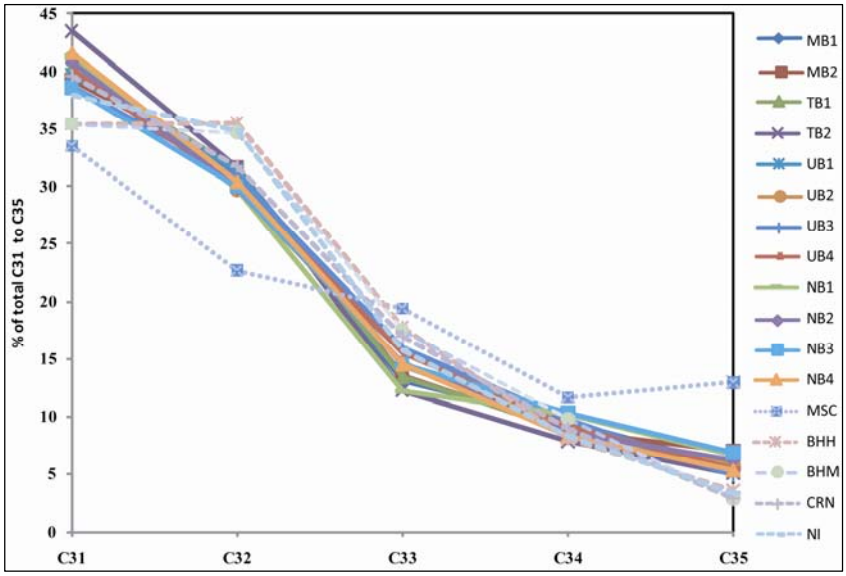

Fig. S6. Hopane distribution in samples and tar ball samples

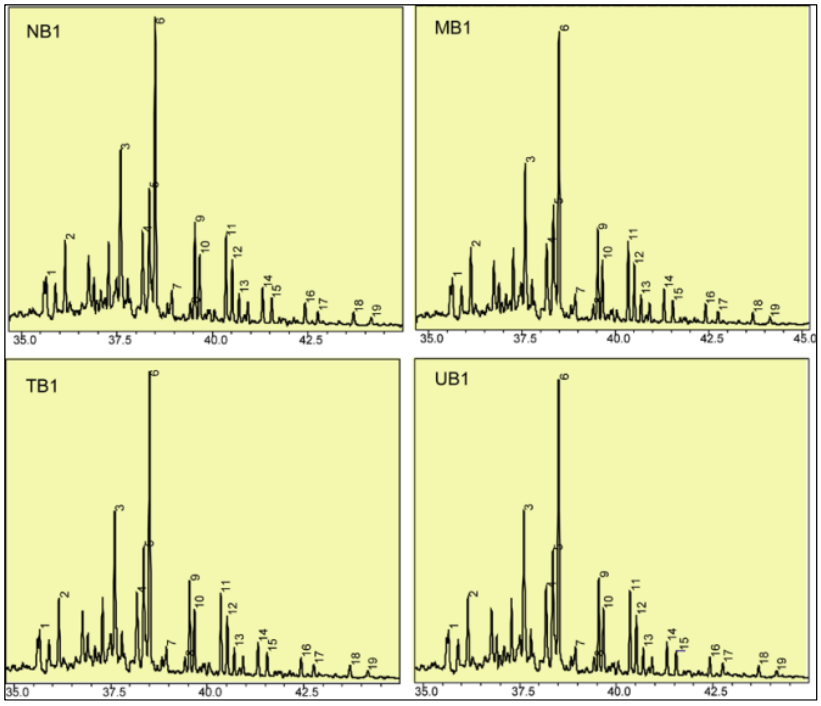

Fig. S7. Hopane chromatograms(m/z-191) for randomly selected tar ball samples

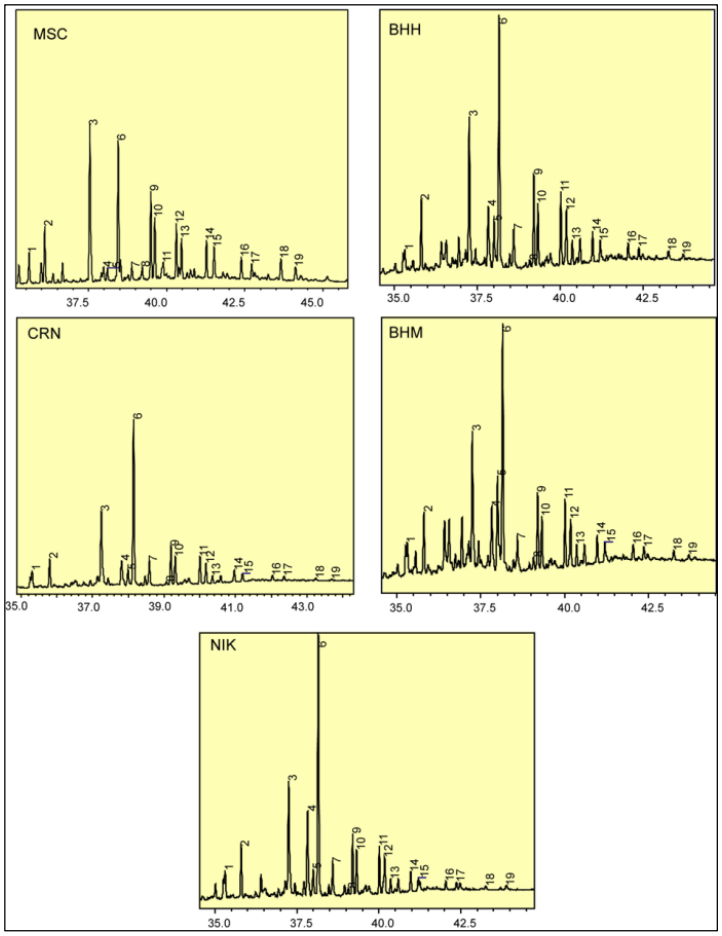

Fig. S8. Hopane chromatograms (m/z-191) for crude oils sample

Fig. S8 shows the compounds of hopanes detected in crude oil samples. Among five crude oils MSC is entirely different than the others. CRN and NIK resembled as same in which the Oleanane is significant, where as BHM and BHH are enriched in Oleanane and resembled almost same. A minor difference between BHM and BHH is, BHM is more abundant in Oleanane than the BHH. The names of the compounds of peaks numbered (1-19) in the Fig. S5 and S6 are given in Table S3.

Table. S6. Hopane DRs.

Sample	C_{29}/C_{30}	$\sum C_{31}$-C_{35}/C_{30}	Tm/Ts	Olea/C_{30}	Ts/Tm	Ts/(Ts+Tm)	C31 R/C30
MB1	0.55	1.15	1.48	0.30	0.68	0.40	0.46
MB2	0.55	1.25	1.29	0.32	0.78	0.44	0.49
TB1	0.47	1.06	1.96	0.28	0.51	0.34	0.42
TB2	0.58	1.27	1.80	0.35	0.56	0.36	0.55
UB1	0.47	1.08	1.79	0.28	0.56	0.36	0.42
UB2	0.49	1.20	1.62	0.29	0.62	0.38	0.47
UB3	0.53	1.33	1.75	0.31	0.57	0.36	0.51
UB4	0.48	1.25	1.58	0.29	0.63	0.39	0.47
NB1	0.57	1.31	1.84	0.34	0.54	0.35	0.55
NB2	0.56	1.39	1.92	0.34	0.52	0.34	0.55
NB3	0.57	1.34	2.23	0.33	0.45	0.31	0.51
NB4	0.49	1.19	1.84	0.29	0.54	0.35	0.47
BHH	0.56	1.40	2.91	0.18	0.34	0.26	0.56
BHM	0.57	1.21	1.86	0.36	0.54	0.35	0.45
NIK	0.52	0.98	1.78	0.11	0.56	0.36	0.39
CRN	0.52	0.90	1.55	0.11	0.64	0.39	0.39
MSC	0.97	2.94	1.52	0.09	0.66	0.40	1.13
MECO1	1.41	1.86	0.35	0.03	n.a	n.a	n.a
MECO2	2.01	1.8	2.31	0	n.a	n.a	n.a
MECO3	1.56	2.3	0.76	0	n.a	n.a	n.a
SEACO1	0.98	0.48	2.2	1.53	n.a	n.a	n.a
SEACO2	0.85	0.41	1.49	1.12	n.a	n.a	n.a
SEACO3	1.16	0.89	1.43	0.3	n.a	n.a	n.a
SEACO4	0.85	0.78	0.52	0.11	n.a	n.a	n.a

C_{29}/C_{30}: Ratio of 7α(H),21β(H)-30-norhopane to 17α(H),21β(H)-hopane

$\sum C_{31}$-C_{35}/C_{30}: Ratio of sum of 17α(H),21β(H) C_{31} homohopane to 17α(H),21β(H) C_{35} pentakishomo hopane relative to 17α(H),21β(H)-hopane

Tm/Ts: Ratio of 17α(H), 22, 29,30-trisnorhopane relative to 18α(H),22,29,30-trisnorneohopane

Olea/C_{30}: Ratio of Oleanane relative to 17α(H),21β(H)-hopane

Ts/Tm: Ratio of 18α(H), 22, 29,30-trisnorneohopane relative to 17α(H),22,29,30-trisnorhopane

Ts/(Ts+Tm): Ratio of 18α(H),22,29,30-trisnorneohopane relative to sum of 18α(H), 22, 29,30-trisnorneohopane and 17α(H),22,29,30-trisnorhopane

C_{31} R/C_{30} Ratio of 17α(H),21β(H)-22R-homohopane to 17α(H),21β(H)-hopane

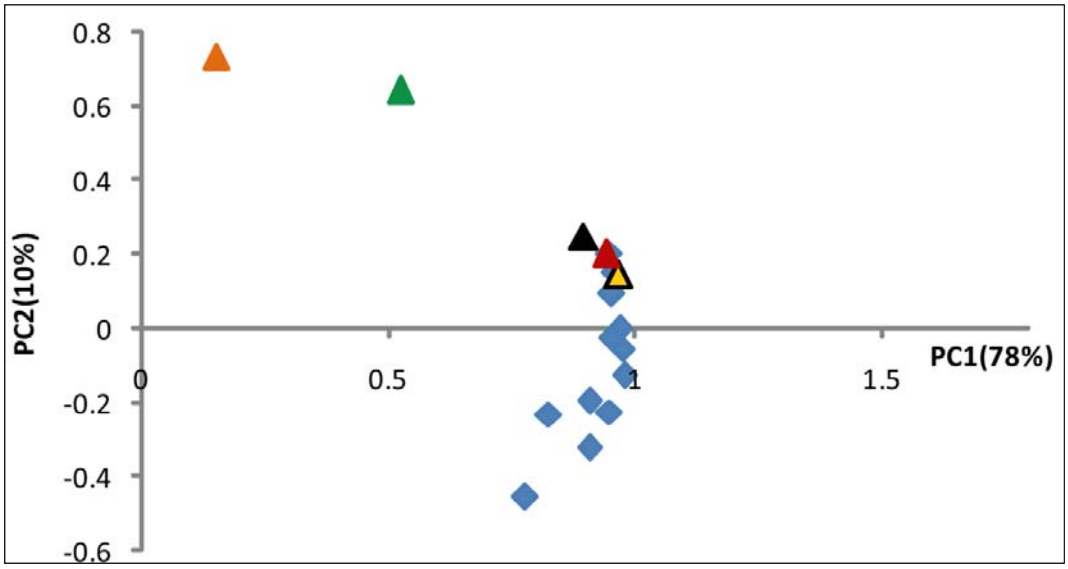

Fig. S9. Observation axes for the first two principal components in tar ball samples (Blue diamond) and crude oils (orange triangle-MSC; green triangle-CRN ; black triangle- NI; red triangle -BHH; yellow triangle- BHM).

Table S3. Names of hopane compounds detected in the samples and crude oils

Peak No.	Compound	Compound Name
1	Ts	18α(H),22, 29,30-trisnorneohopane
2	Tm	17α(H),22, 29,30-trisnorhopane
3	αβ-29	17α(H), 21β(H)-30-norhopane (normoretane)
4	αβ-30N	17β(H), 21α(H)-30-norhopane (normoretane)
5	Oleanane	18α(H) and 18β(H)
6	C_{30} αβ	17α(H),21β(H)-hopane
7	C_{30} βα	17β(H),21α(H)-hopane
8	C_{31} αβ-S	17α(H),21β(H)-22S-homohopane
9	C_{31} αβ-R	17α(H),21β(H)-22R-homohopane
10	C_{31} βα-R	17β(H),21α(H)-22R-homohopane
11	C_{32} αβ -S	17α(H),21β(H)-22S-bishomohopane
12	C_{32} αβ -R	17α(H),21β(H)-22R-bishomohopane
13	C_{32} βα -R	17β(H),21α(H)-22R- bishomohopane
14	C_{33} αβ	17α(H),21β(H)-22S-trishomohopane
15	C_{33} βα	17 β(H),21α(H)-22R-trishomohopane
16	C_{34} αβ	17α(H),21β(H)-22S-tetrakishomohopane
17	C_{34} βα	17β(H),21α(H)-22R-tetrakishomohopane
18	C_{35} αβ	17α(H),21β(H)-22S-pentakishomohopane
19	C_{35} βα	17 β (H),21α(H)-22R-pentakishomohopane

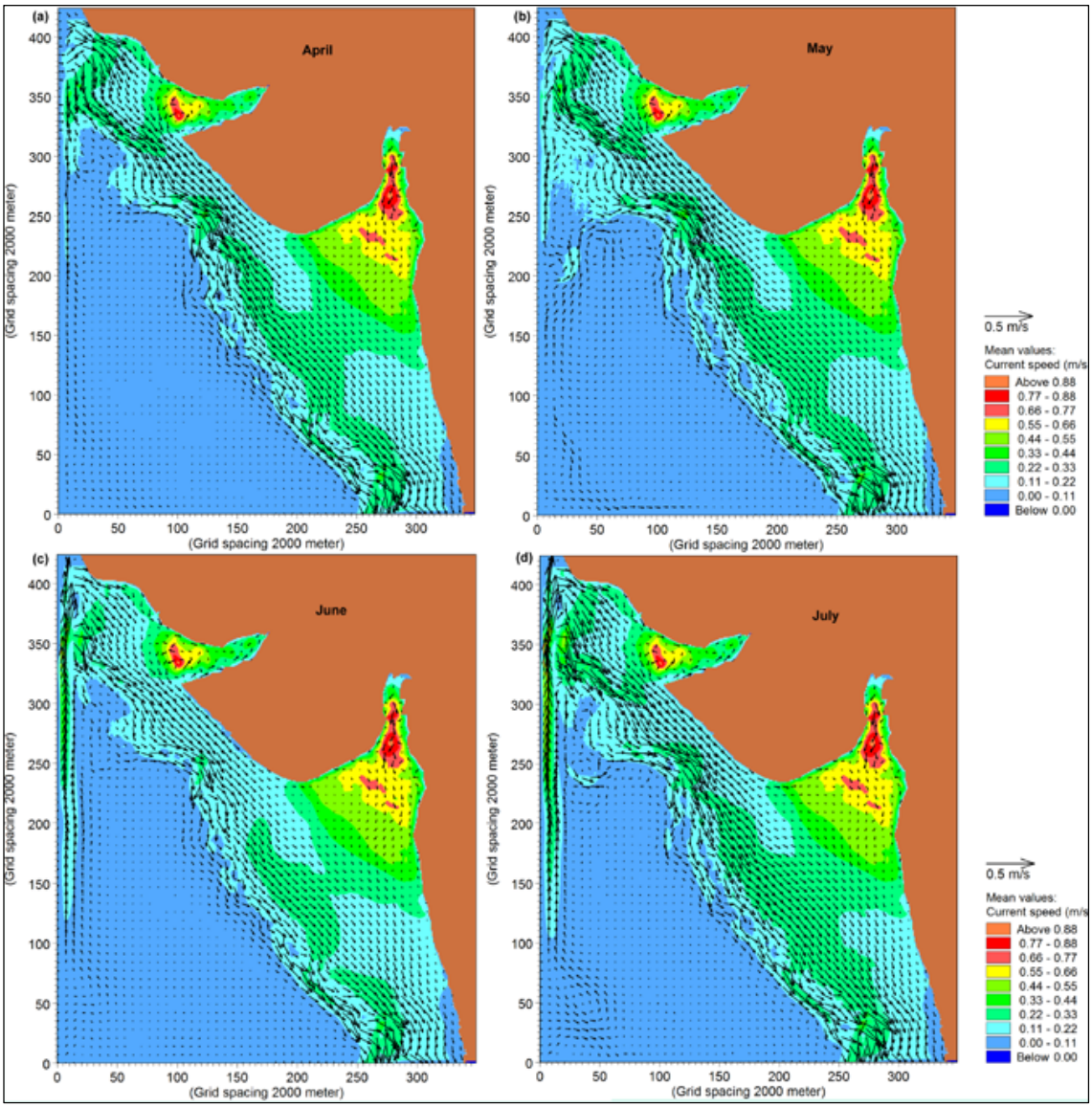

Fig. S10. Monthly averages of modeled currents for: (a). April, (b) May, (c) June and (d). July

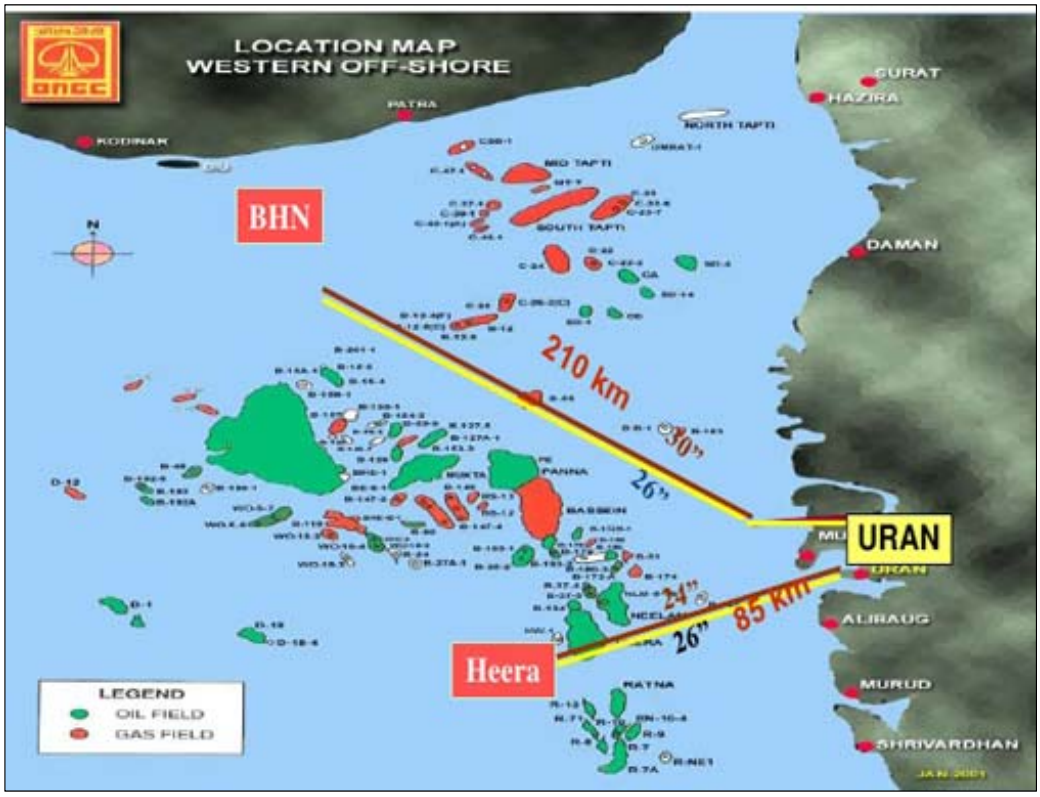

Fig. S11. Location of BH oil fields and Uran plant (Courtesy: ONGC)